TECHNICAL REPORT

70-26-AD

WIND EFFECT ON GLIDING PARACHUTE SYSTEMS WITH NON-PROPORTIONAL AUTOMATIC HOMING CONTROL

by

Thomas F. Goodrick

November 1969

UNITED STATES ARMY
NATICK LABORATORIES
Natick, Massachusetts 01760

Airdrop Engineering Laboratory

67

This document has been approved for public release and sale; its distribution is unlimited.

Citation of trade names in this report does not constitute an official indorsement or approval of the use of such items.

Destroy when no longer needed. Do not return to the originator.

This document has been approved
for public release and sale;
its distribution is unlimited.

AD_____

TECHNICAL REPORT
70-28-AD

Wind Effect on Gliding Parachute Systems with Non-Proportional Automatic Homing Control

by

Thomas F. Goodrick

Project Reference:
1F162203D195

November 1969

Airdrop Engineering Laboratory
US Army Natick Laboratories
Natick, Massachusetts 01760

FOREWORD

This report presents the results of a short-term study undertaken to fill a gap in a rapidly developing technology of gliding parachute systems. While the problem is not very complex, it is hoped that a concise presentation of the equations and illustrative calculations will be of value.

The author wishes to express his appreciation to Mr. Richard J. Greene whose competent preparation of the illustrations facilitated timely completion of the study.

This study was conducted under Department of the Army Project No. 1F162203D195, Exploratory Development of Airdrop Systems.

CONTENTS

TABLES

ILLUSTRATIONS

ABSTRACT

Equations are presented and evaluated for estimating the wind effect on the approach path and descending orbit of gliding parachute systems with non-proportional automatic homing control. Exact equations are presented for calculating the overall downwind displacement, the total time, and the positions of four characteristic points on a typical descending orbit, or complete circuit, over the target. Iteration equations are presented incorporating homing simulations for calculating positions at equal time intervals on the initial approach and descending orbit. The control response time, effect of variations in deployment position, and impact probability are discussed. The equations are evaluated for systems having horizontal velocities of 40 and 60 fps and having turn radii of 75 and 100 ft in wind speeds of from 4 to 32 fps.

Based on results of a computer study, empirical equations are presented for calculating the probability of impact within a given radius of the target and for calculating the radius of the circle of equal probability as functions of turning radius, wind velocity, and horizontal system velocity relative to air (or glide ratio assuming standard airdrop descent velocity). The analysis shows that increasing horizontal system velocity relative to air decreases wind distortion both of a crosswind approach and of the descending orbit thereby increasing the probability of impact close to the target.

1. Introduction

a. Purpose

The practical design of gliding parachute systems requires estimation of performance in a wind while the system is under automatic-homing radio control. While most gliding systems would have a manual control capability which would allow a man on the ground to correct for wind effects, automatic control should be sufficiently accurate to facilitate use by relatively untrained and inexperienced field personnel and to facilitate use in limited visibility. Most gliding parachute systems have glide ratios from 2.0 to 3.0 and have a rate of descent of about 20 ft/sec. Therefore, the horizontal velocity component is generally between 40 and 60 ft/sec. A typical wind speed of 15 knots or 25 ft/sec would have a significant effect on the ground track of such systems. This report presents both basic equations for determining certain ground track characteristics and an extensive computer study which shows the quantitative effects of various system parameters on the ground track in a wind. Also, an empirical equation is presented for use in design of the control system to satisfy given performance requirements.

b. Scope of the Analysis

The analysis is based on a non-proportional radio control system which would initiate control only for a full left turn, full right turn, or straight flight depending on orientation of the system toward the transmitter which is located at the target point. This system is less expensive and mechanically simpler than a proportional system. Also, the author is aware of one control system of this type currently in experimental use.

Equations are presented in this paper both for calculating certain characteristic points on the final descending orbit and for computing instantaneous points on the approach. Simple analyses of velocity vectors and geometry are used to calculate points on a descending orbit and the time for one complete orbit, or circuit, over the target. By considering small, time increments during controlled turns, the ground track during homing approach and descending orbits can be approximate. A basic estimate of the deployment envelope for an offset delivery mission is presented to show the range of possible error in altitude of the system at the completion of the initial approach to the target. Based on the assumption that impact will occur any time during a typical descending orbit over the target, impact position probability is considered equal to the time spent within a given distance of the target in percent total time for a complete orbit.

2. Methods of Analysis

Effects of wind on the performance of gliding systems must be analyzed from the concept that the system has a constant total velocity relative to the air regardless of wind. When the system executes a constant-rate turn for a given amount of time, the change in its position over the ground may be determined by calculating the position it would have without wind and then displacing the position downwind a distance equal to the product of the steady wind speed and the elapsed time. Orientation of the system is parallel to the orientation it would have without wind.

a. Basic Orbit Geometry

Four characteristic points and the total time of the typical descending orbit can be calculated from exact relations. The results apply accurately to the second and subsequent passages over the target which are independent of the initial approach. Consider the geometric relations shown in Figure 1 where V is the horizontal velocity component of the system relative to air, W is the wind speed (parallel to the Y-axis) and r is the radius of the turn of the system in calm air. Circular motion to the left of the Y-axis is assumed. The positions relative to the X-axis and the time relationships of the four points on the actual orbit are derived from the positions on an analogous circular orbit.

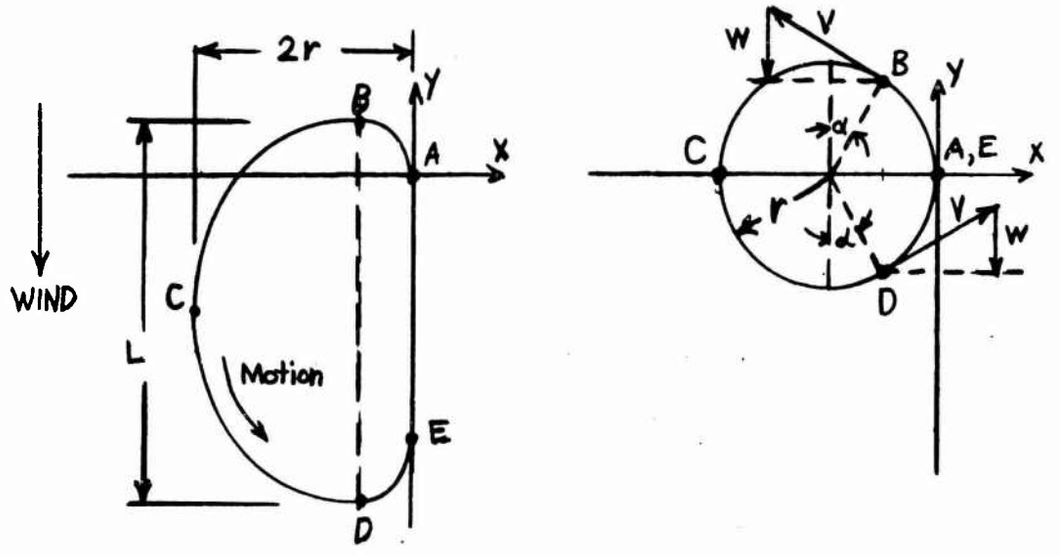

a) Actual Orbit b) Analogous Circular Orbit

Fig 1. BASIC GEOMETRIC RELATIONS FOR DESCENDING ORBIT

Point A coincides with the target. On a typical orbit, the system would head upwind at Point A and hold a constant turn control through Points B,C,D and E to return to Point A. At Point B, the vector sum of the system velocity and the wind velocity yields a resultant having pure crosswind direction. Hence

$$\sin\alpha = W/V \tag{1}$$

or

$$\alpha = \arcsin W/V \tag{2}$$

where α is the angle of inclination of the vector V from the x-axis. From the geometry related to a circle, we see that α is also the angle from the diameter parallel to the Y-axis of a line passing through the point on the circle analogous to Point B. The angularity of the vector V thus changes by the amount $\pi/2 - \alpha$ between Point A and Point B. If T_o is the time required to turn a complete circle in calm air, then $T_o (\pi/2 - \alpha) /2\pi$ is the time required to move from Point A to Point B. The coordinates of Point B may thus be calculated from the relations

$$X_B = -r (1 - \sin\alpha) \tag{3}$$

$$Y_B = r \cos\alpha - WT_o (\pi/2 - \alpha) /2\pi \tag{4}$$

At Point C, motion is purely downwind. The coordinates of Point C are

$$X_C = -2r \tag{5}$$

$$Y_C = -WT_o/2 \tag{6}$$

where the system has cojplated a 180-degree turn. At Point D, the system has an upwind velocity component sufficient to cancel the wind velocity. The coordinates of Point D are

$$X_D = X_B \tag{7}$$

$$Y_D = -r \cos\alpha - WT_o (3\pi/2 + \alpha) /2\pi \tag{8}$$

At Point E, motion, is again, purely upwind toward the target. The x coordinate of Point E is zero, and the y coordinate is

$$y_E = -WT_o \tag{9}$$

The total distance from Point B to Point D is

$$L = 2r \cos\alpha + WT_o (\pi + 2\alpha) /2\pi \tag{10}$$

The total elapsed time for the complete orbit is

$$T = T_o + |y_E| / (V-W) \tag{11}$$

or, substituting the value of y_E from Eq (9),

$$T = T_o + WT_o / (V-W) \tag{12}$$

The value of T_o may be calculated from

$$T_o = 2\pi r/V \tag{13}$$

This value may be substituted into each of the above equations involving T_o to give the following simplified relations:

$$y_B = r \cos\alpha - r\,(W/V)\,(\pi/2 - \alpha) \tag{14}$$

$$y_C = -\pi r\,(W/V) \tag{15}$$

$$y_D = -r \cos\alpha - r\,(W/V)\,(3\pi/2 + \alpha) \tag{16}$$

$$y_E = -2\pi r\,(W/V) \tag{17}$$

$$L = 2r \cos\alpha + r\,(W/V)\,(\pi + 2\alpha) \tag{18}$$

and

$$T = 2\pi r/(V-W) \tag{19}$$

Note that, in each geometric relation, the sole velocity term is the dimensionless ratio W/V. It is interesting that the time for a complete orbit in a wind is equal to the time required to turn a perfect circle at the minimum ground speed, V - W. For gliding parachute systems, values of W/V may commonly be of the magnitude of 1/2. Hence, the above equations show that significant distortions of the calm air orbit may commonly occur.

The four characteristic points, the overall length, and the orbit time are sufficient for basic estimation of wind effects. However, for any time, t, during an orbit, the position of the system can be determined from the following equations:

For $0 \leq t \leq T_o$,

$$x = -r\,(1 - \cos\,(Vt/r)) \tag{20}$$

$$y = r \sin\,(Vt/r) - Wt \tag{21}$$

and, For $T_o < t \leq T$, $x = 0$ and

$$y = -WT_o + (t - T_o)\,(V-W) \tag{22}$$

However, for calculating instantaneous positions, the equations presented below in Section 2b are more suitable since they apply to the approach as well as to the descending orbit.

From the basic relations, we see that distortion increases in direct proportion to r and in inverse proportion to V and, hence, to the glide ratio. Maximum glide ratio would, therefore, minimize distortion for a given radius of turn.

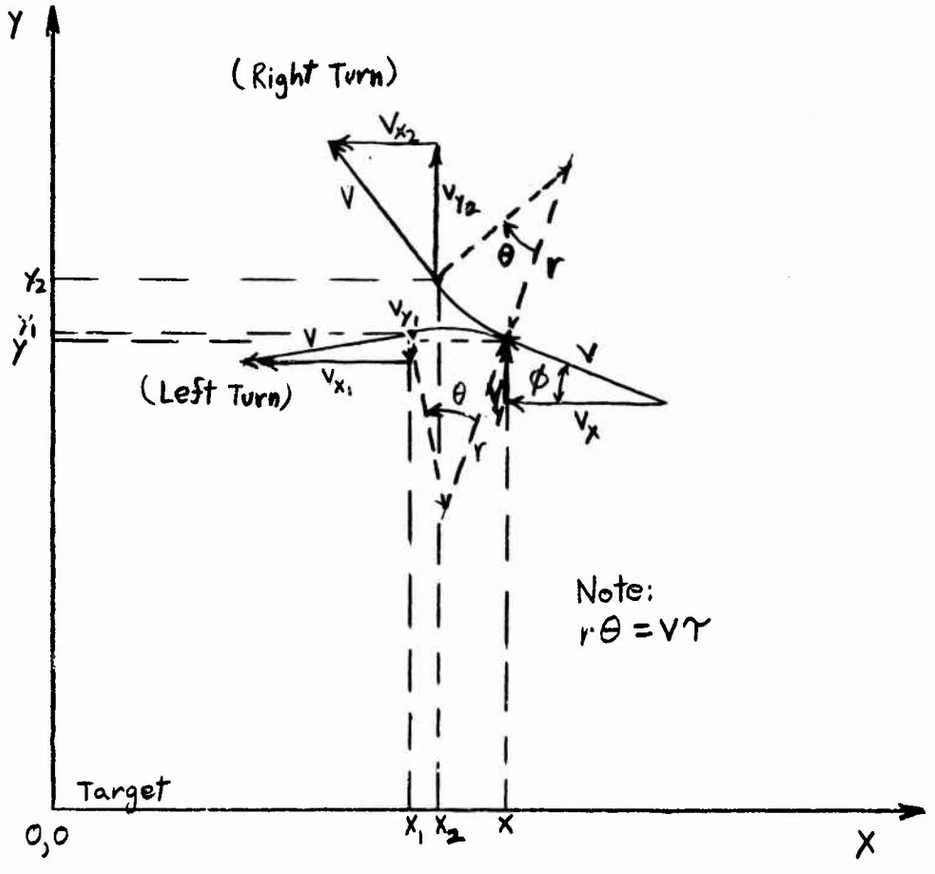

Fig 2. GEOMETRY OF TURN DURING APPROACH (WITHOUT WIND DISPLACEMENT)

b. Iteration Equations for Homing

Points at small time intervals along the path of the homing approach may be determined from the assumption that, at any position, the system can turn through a small arc of angle θ either to the left or to the right - whichever brings it closer to the target. Geometric relations are derived first for the case of calm air. The wind effect is added as a constant displacement at the end of each arc. The

tangential velocity is equal to the constant horizontal velocity of the system since the system has aerodynamic equilibrium. Actually, the velocity and glide ratio may be less in a turn than in straight flight. However, it will be shown later that straight flight is virtually impossible for the assumed control system. Hence, the velocity may be considered constant. From the geometry shown in Fig 2, the position and orientation of the system upon completion of the arc θ may be calculated exactly.

Assume the radius of turn, r, the arc angle, θ, and the horizontal velocity component, V, relative to air remain constant. Given an initial position, (x,y), and initial velocity components, V_x and V_y, which indicate orientation relative to the target at the origin of the coordinate system, the two possible end points (x_1, y_1) and (x_2, y_2) after completing a left or right turn through angle, θ, may be calculated from the relations

$$x - x_1 = 2r \sin(\theta/2) \cos(\phi - \theta/2) \quad (23)$$

$$-(y - y_1) = 2r \sin(\theta/2) \sin(\phi - \theta/2) \quad (24)$$

$$x - x_2 = 2r \sin(\theta/2) \cos(\phi + \theta/2) \quad (25)$$

$$-(y - y_2) = 2r \sin(\theta/2) \sin(\phi + \theta/2) \quad (26)$$

where ϕ is the initial angle of inclination of V from the x-axis. The velocity components at points (x_1, y_1) and (x_2, y_2) may be calculated from

$$V_{y_1} = V \sin(\phi - \theta) \quad (27)$$

$$V_{x_1} = V \cos(\phi - \theta) \quad (28)$$

$$V_{y_2} = V \sin(\phi + \theta) \quad (29)$$

$$V_{x_2} = V \cos(\phi + \theta) \quad (30)$$

The angle of ϕ has the relations

$$\sin \phi = V_y/V \quad (31)$$

$$\cos \phi = -V_x/V \quad (32)$$

Where V_y and V_x are the values prior to the turn.

If S_1 and S_2 are the squares of the distances from the origin to points (x_1, y_1) and (x_2, y_2) as defined by

$$S_1 = x_1^2 + y_1^2 \tag{33}$$

$$S_2 = x_2^2 + y_2^2 \tag{34}$$

then homing control is effected by choosing the shorter distance on the basis of the sign of $S_2 - S_1$. After algebraic manipulation of Eq (23), (24), (25) and (26) we find that the sign of $S_2 - S_1$ is dependent on the sign of $xV_y - yV_x$. Thus if

$$xV_y - yV_x > 0,$$

than

$$S_2 - S_1 > 0;$$

and if

$$xV_y - yV_x \leq 0,$$

than

$$S_2 - S_1 \leq 0.$$

In final form, the equations for the coordinates x' and y' of the end point of the arc and the corresponding velocity components V_x' and V_y' are given by

$$x' = x + (2r/V) \sin(\theta/2) \left[V_x \cos\frac{\theta}{2} - aV_y \sin\frac{\theta}{2}\right] \tag{35}$$

$$y' = y + \frac{2r}{V} \sin\frac{\theta}{2} \left[V_y \cos\frac{\theta}{2} + aV_x \sin\frac{\theta}{2}\right] - W\tau \tag{36}$$

$$V_x' = V_x - 2 \sin\frac{\theta}{2} \left(V_x \sin\frac{\theta}{2} + aV_y \cos\frac{\theta}{2}\right) \tag{37}$$

$$V_y' = V_y + 2 \sin\frac{\theta}{2} \left(aV_x \cos\frac{\theta}{2} - V_y \sin\frac{\theta}{2}\right) \tag{38}$$

where $a = +1$ if $(xV_y - yV_x) > 0$

and $a = -1$ if $(xV_y - yV_x) \leq 0$.

These equations may be used in an iterative calculation to find all subsequent points on the ground track during the approach and the final descending orbit. The sole correction for wind effects is made by subtracting the term $W\tau$ from the y coordinate as shown in Eq (36) where τ is the time elapsed during the turn. Values of V_x' and V_y' are relative to air and remain unaffected by wind. Hence, the values of x', V_x', V_y' and the corrected value of y' may be used to determine the value of a for the subsequent turn.

The angle $\theta/2$ may be calculated in terms of the time increment by the relation

$$\left(\frac{\theta}{2}\right) = 180V\tau/2\pi r \tag{39}$$

for $\theta/2$ in degrees.

c. Significance of the Iterating Increment

In specific applications, the value of τ used in Eq (39) may be chosen to represent a characteristic response time of the parachute system. Prior to a turn, the physical parachute system must undergo a lateral oscillation governed by system geometry and by the effective masses of the canopy and of the suspended load. While a detailed analysis of this phenomenon is beyond the scope of this report, general considerations show that the period of the oscillation is a function of parameters which would remain virtually constant throughout gliding flight. The analysis presented in the report "Dynamic Stability of a Parachute Point-mass Load System" by H.G. Heinrich and L.W. Rust Jr.[1] shows comparable dynamic relations. A similar analysis could be used to estimate the response time of a gliding system to a turn control. If the response time for a particular system can be determined, the use of such a value for the iterating increment of time, τ, in Eq (39) would increase the accuracy of the computed ground track. The physical system would be capable of executing homing control only at equally spaced time intervals according to the oscillatory motion.

For the computer evaluation presented in this report, the values of τ range from 0.3 to 2.4 sec. This range seems reasonable in view of the known characteristics of standard vertically-descending parachute systems. For example the time required for a system consisting of a 5,000 lb. payload and 100-ft. diameter circular canopy to rotate from 27° to 0° vertical inclination is approximately 2.3 sec as shown by flight test data. Personnel parachutes exhibit similar oscillation times. However, the values of τ used in this computer study were calculated as 4, 8 and 16% T_o to give incremental turns of 14.5, 29 and 58 degrees. Values of τ less than 4% T_o required impractical computation times and did not result in significantly smoother homing patterns as discussed in section 3a. For values of τ greater than 16% T_o and approaching 25% T_o, the computational methods of section 2b show adverse peculiarities. The assumption that the track remains circular during the time τ is probably invalid for larger values of τ, since the actual path is somewhere between a straight tangential line and a pure circular arc during the oscillatory motion.

---

(1) Report No FDL-TDR-64-1[illegible] (June 1965) USAF Flight Dynamics Laboratory, WPAFB, Ohio.

d. Effect of Deployment Envelope

The range of variation in altitude of the gliding system as it first arrives over the target shows that, in general, several orbits or 360-degree turns will be completed before impact. Obviously, if the deployment position could be controlled sufficiently, ground impact would occur at the target regardless of the orbit dimensions since final orbiting could be avoided. Although the glide ratio, ℓ/d, in aerodynamic equilibrium is constant, random wind variations and random system orientation during deployment must be assumed for a mission which utilizes the full offset capability of the gliding system. Surface winds will seldom be constant between the launch and target positions. Let ΔW be the maximum random wind velocity which may occur either toward, or away from, the target. Then the effective glide ratio has the range of from

$$(\ell/d)_{min} = \frac{V - \Delta W}{Vd} \tag{40}$$

to

$$(\ell/d)_{max} = \frac{V + \Delta W}{Vd} \tag{41}$$

where V_d is the constant rate of descent and V is the constant horizontal velocity relative to air. Navigational error, varying loss of altitude during deployment, and random orientation of the system at completion of deployment will contribute to uncertainty in range and altitude at the instant the system starts gliding directly toward the target. While a complete analysis of these factors is beyond the scope of this report, assume the range is $\ell_o \pm \Delta\ell$ and $h_o \pm \Delta h$ is the altitude when the system is fully deployed and initially oriented toward the target. The variation in altitude at the first pass over the target will then be approximately between

$$h_{min} = (h_o - \Delta h) - (\ell_o - \Delta\ell)\left(\frac{V_d}{V - \Delta W}\right) \tag{42}$$

and

$$h_{max} = (h_o + \Delta h) - (\ell_o + \Delta\ell)\left(\frac{V_d}{V + \Delta W}\right) \tag{43}$$

This assumes that launch is at a prevailing upwind location since a crosswind approach would be subject to additional variations. To plan a typical offset mission for the gliding system, a value of ℓ_o would probably be chosen on the basis of tactical requirements. Values of Δh, $\Delta\ell$, V_d, V and ΔW would be known or estimated. A suitable value of h_o, could be found from Eq (42) assuming $h_{min} = 0$. Then the corresponding value of h_{max} is

$$h_{max} = 2\Delta h + 2 V_d \frac{(\Delta W \ell_o + V \Delta \ell)}{(V + \Delta W)(V - \Delta W)} \quad (44)$$

and the median altitude is

$$\bar{h} = \Delta h + V_d \frac{(\Delta W \ell_o + V \Delta \ell)}{(V + \Delta W)(V - \Delta W)} \quad (45)$$

To determine the order of magnitude of $\bar{h}$ consider the following sample values:

ℓ_o = 35,000 ft.
$\Delta \ell_o$ = 500 ft.
Δh_o = 300 ft.
V = 60 fps
V_d = 20 fps
ΔW = 20 fps and 0

For ΔW = 20 fps, Eq (45) gives the value $\bar{h}$ = 4,862 ft with h_o = 17,550 ft from Eq (42). If we assume the radius of turn, r, is 100 ft, Eq (19) gives the value T = 15.6 sec. With V_d = 20 ft. the altitude loss per orbit is 312 ft. The high value of h is mostly a function of ΔW since h = 467 ft for ΔW = 0. Thus, we see that an average of from 1.5 to 15.6 complete orbits would be executed prior to impact for ΔW between 0 and 20 fps. Therefore, impact accuracy is largely dependent on the orbit geometry.

e. Impact Position Probability

The analysis of the previous section shows that, in general, impact may occur at any time during a typical orbit over the target. In other words, impact will occur at equal probability with time during an orbit. Hence, the probability that the system will impact within a given radius of the target is equal to a ratio of time spent within the radius to the total time elapsed for a typical orbit. For the computer study presented in Section 3, impact probability is calculated from the number of points, indicating equal time increments, which are found within a given radius of the transmitter (i.e. - the origin of coordinates) as a percent of the total number of points for a complete orbit. By plotting the probability as a function of radius from the target, an estimate of the radius of the circle of equal probability (CEP) is obtained. An attempt was made, using the equations of Section 2a, to derive an approximate equation for the radius of the CEP since the parameter is commonly used to indicate impact accuracy and is of prime importance in determining the size of the drop zone required by a gliding system. No practical approximation was found from these equations. However, the recurring appearance of the dimensionless terms R_c/r and W/V - where R_c denotes radius of the CEP - prompted an empirical analysis of the computer results in relation to these parameters. A suitable empirical equation was thus obtained. Techniques and results are presented fully in Section 3d.

3. Results of Computer Study

A computer study was made of the relations presented in Section 2b (Fig 3). The ground track was computed from the initial point until completion of two orbits or until a complete orbit was clearly defined. Although actual impact position would depend on the altitude at the initial point, the system would follow the computed ground track prior to impact regardless of altitude providing glide ratio and wind speed did not change due to altitude effects. In all cases the wind was assumed constant at the specified speed directed toward the target along the positive y - axis.

Comparison was made between the iteration results and the geometric relations presented in Section 2a. Impact probability was estimated according to the hypothesis discussed in Section 2e.

a. Cases Studied

The cases studied, as described in Table 1, may be considered typical of most gliding parachute systems. A wind speed of 15 knots, or 25 fps, is assumed for Cases 1 - 18 as a standard maximum operating condition. Since cargo safety during impact generally requires a rate of descent of 20 fps, horizontal velocities relative to air of 40 to 60 fps were chosen to exemplify the common range of glide ratio from 2.0 to 3.0. Values of the radius of turn were chosen as 75 and 100 ft. which are reasonable in terms of aerodynamic performance and practical accuracy requirements. However, gliding systems for payloads beyond 1000 lb will probably have larger turn radii since the turn radius is somewhat related to the distance between the canopy and the payload. Values for the time lag, τ, or iterating time increment, were chosen as 4%, 8% and 16% of the total time, T_o, to turn 360 degrees in calm air. In one case, not included in the final presentation, a value of τ = 0.4% of T_o was used. However, the results differed negligibly from those for τ = 4% T_o, and computation time was extremely long. For cases 1-9, comparison is made between approaches near the target from upwind, crosswind, and downwind positions. All remaining cases show either the approach from upwind or the orbit from an initial position over the target.

Cases 1 - 21 were studied primarily to observe performance near the target. The effect of wind on crosswind approaches was also studied for offset distances of up to 2,000 ft. Parameters considered for the crosswind approaches are initial offset distance, time lag, glide ratio, and radius of turn. System characteristics are the same as in the cases studied near the target. No provision was made for a cone of silence over the transmitter.

b. Observations

The computed ground track for the calm air condition is shown in Figure 4. Figures 5 to 23 show the effects of wind for Cases 1 to 18 as listed in Table 1. Figures 5,8 and 12 show that an approach from an initial position upwind of the target causes the system to execute a small orbit between the first and second passes over the target. In some figures an oscillating curve has been drawn through points which seem to lie on a stright line. The slope of the oscillating curve coincides with the system orientation at each point as determined from the velocity vectors V_x and V_y. This is indicative of the type of motion although the exact amplitude is not known. Indeed, oscillating orientation is not necessarily indicative of an oscillatory path over the ground. The figures where τ = 8% and 16% T_o show some pecularities resulting from the discrepency between actual system orientation and the apparent direction of the ground track. Figure 11 shows the actual system orientations indicated by the resultant of V_x and V_y for an expanded portion of the ground track of Case 6. The portion shown in Figure 11 occurs during the second approach to the target shown in Figure 10. The longer time lags in several instances cause short oscillations at close proximity to the target as exemplified in Figures 11,12,14 and 20. Indeed, a peculiar resonance is shown in Figures 14 and 20 which would greatly increase the probable accuracy. This phenomenon would seem, however, difficult to achieve and control in practice. In each of the figures, a circle of 200 ft radius is shown for comparison to the calm air accuracy with r = 100 ft.

Figures 24,25 and 26 show the effect of wind on long crosswind approaches. For various offset distances up to 2,000 ft with the system values of Case 8, the initial approach to the target is consistently from the five-o'clock direction. Maximum downwind displacement increases from the value for a 500 ft offset at a rate of 15 ft per 100 ft additional offset (Fig 24). This rate is proportional to W/V, however. The path for a small time lag (Fig 25) is virtually the mean of the path for the larger time lag.

Downwind drift on the approach is much more sensitive to glide ratio than to radius of turn assuming a constant rate of descent. Since most gliding systems experience a loss of glide ratio as radius of turn is decreased, the important feature of Figure 26 is that a horizontal velocity with large radius of turn may yield less distortion than a lower horizontal velocity with smaller radius of turn. The large time lags were used in Figures 24 and 26 purely for shorter computation times.

c. Correlation with Basic Orbit Geometry

The values of W,V, and r for Cases 1 to 18 were used in the equations of Section 2a to calculate the maximum downwind displacement (L), the total elapsed time (T) per orbit and the coordinates of the four characteristic points (B,C, D, and E) for typical orbits corresponding to the computed ground tracks. The calculated results are compared to the measured values from Cases 1,2,3,10,13 and 16 in Tables 2A and 2B. The actual values as determined from Figures 6,7,8, 16,19 and 22 are shown in Table 2A for comparison to the calculated values. The measured values of L and T have good correlation with the calculated values while the other values appear to have poor correlation in several cases. However, Table 2B shows that the apparent position discrepancy is the result of delays in the start of the orbits due to inefficient homing commands when the system passes over the target. The values for each case shown in Table 2B were obtained from the corresponding values in Table 2A by adding constant displacements to the point coordinates so that Point B was made coincident with the calculated position. The resulting correlation of Points C, D and E is very good.

When the system returns to the target, it generally passes over the target during one time increment. Hence, the orientation of the system after passing the target is dependent on the homing control exerted at the beginning of the time interval before passing the target. Although the theoretical orbit is the result of a constant rate turn in one direction, the system orientation at the end of a time interval may dictate a homing turn in the opposite direction because of close proximity to the target. The inconsistency, therefore, of one or two turns in opposite directions results in an upwind displacement of the point at which the system commences a constant rate 360-degree turn.

d. Effect of Parameters on Impact Position Probability

The effect of approach direction and time lag on impact accuracy related to a 200 ft radius circle for Cases 1-9 is shown in Table 3. The important observations from Table 3 are that probability during the first orbit is best from an upwind approach and that probability generally increases with time lag. Figures 12 and 14 illustrate the behavior near the target accounting for the listed probabilities of 100%.

For Cases 1,10,13 and 16 in which $\tau = 4\%\ T_o$, probabilities were determined for target circles of 50,100,150,200,250,300 and 350 ft radius. The radii of the circles of equal probability (i.e. - 50% probability) were determined from a graph of probability vs radius from target. The results showed peculiar

relations and a high degree of linearity which warranted further study. Hence, three more cases, Cases 19, 20 and 21 of Table 1, were computed to extend the range of wind velocity studied. Figure 28 shows the resulting ground tracks. The results of the subsequent analysis are shown in Table 4. Since high dependence on the dimensionless values R/r and W/V was anticipated, the results shown in Table 4 were retabulated in Table 4 according to R/r and W/V. The results from Table 5 are plotted in Figure 29 with corresponding least squares linearizations at each value of W/V. To obtain an empirical equation relating probability (P) to R/r and W/V, a linear least squares analysis was made of the variation with W/V of the slopes (m) and of the intercepts (b) for each P vs R/r linearization. The analysis is illustrated in Figure 30 which shows only limited conformity to the linear results. However, as a first approximation, the linear least squares method may be considered sufficient. The resulting empirical function is

$$P = (-35.477 \frac{W}{V} + 45.085) \frac{R}{r} + (29.735 \frac{W}{V} - 10.374) \qquad (46)$$

or

$$P = 45.085 \frac{R}{r} - 35.477 \frac{R}{r} \frac{W}{V} + 29.735 \frac{W}{V} - 10.374 \qquad (47)$$

where P is the percent probability, R is the radius from the target, r is the turning radius, W is the wind speed and V is the horizontal system velocity relative to air. If we let P = 50%, we can solve Eq (47) for the radius of the CEP, R_c:

$$R_c/r = \frac{60.374 - 29.735\ W/V}{45.085 - 35.477\ W/V} \qquad (48)$$

or

$$R_c/r = \frac{1.70 - 0.84\ W/V}{1.27 - W/V} \qquad (49)$$

The curves from Eq (47) superimposed on the data in Figure 27 show particularly good agreement at p = 50%. Therefore, the linear approximations yield sufficient accuracy as resolved in Eq (49). A plot of Eq (49) is presented in Figure 31, $0 \leq W/V \leq 1.0$. Good agreement with theory is found at the end point, W/V = 0 and W/V = 1.0. For W/V = 0, the orbit is a pure circle of radius r passing over the target. Hence, the position is evenly distributed with time about the circle, and the value of R_c is $r\sqrt{2}$ or $R_c/r = 1.41$. Eq (49) gives the value $R_c/r = 1.35$, a difference of 5%. For W/V = 1.0 which has no real significance except in the concept of a mathematical limit, Eq (49) gives $R_c/r = 3.18$. A reasonable assumption for the limit of R_c as W/V approaches 1.0 is $y_D/2$. The value of y_D given by Eq (16) of Section 2a is $-2\pi r$ which is also the value of y_E. Hence, theoretically $R_c = \pi r$ and $R_c/r = \pi = 3.14$. The result of Eq (49) differs by 1%.

Thus, it may be presumed that Eq (49) is an accurate method for determining the radius of the CEP. Then, if R_c, W and V are considered design requirements for the system, the solution of Eq (48) for r,

$$r = R_c \frac{(1.27 - W/V)}{1.70 - 0.84\ W/V} \tag{50}$$

gives the necessary turning radius for the system.

4. Conclusions

The coordinates of four characteristic points and the total downwind displacement defining the geometry of a typical descending orbit can be calculated directly as functions of turning radius and the ratio of wind velocity to horizontal system velocity relative to air (Eq's 2,3,5,7 and 14-18). The total time elapsed per orbit, is equal to the time required to turn a complete circle in calm air at a speed equal to the minimum ground speed in a wind (Eq 19). Points at equal time intervals along the ground track may be computed (Eq's 35-39) with the time interval chosen as a function of the oscillation of the system. Thus, effects of the real system may be approximated. Analysis of the deployment envelope shows that, in general, the median altitude (Eq 45) of the system at the first pass over the target is sufficient to ensure more than one complete orbit prior to impact for missions utilizing the offset delivery capability. Hence, the assumption that the target zone is dependent on orbit geometry is valid. Impact position probability may, therefore, be estimated according to the hypothesis that impact will occur at equal probability with time during a typical orbit.

Computer iterations show good agreement with basic geometric relations, but also show that the magnitude of the time increment may have a significant effect on calculated behavior near the target. Downwind drift during long crosswind approaches increases linearly with offset distance and is inversely proportional to glide ratio while somewhat directly proportional to turning radius.

The linearity of probability values determined from computer results allows accurate empirical formulation of the relation of probability to radius from target, turning radius, wind velocity, and horizontal system velocity (Eq 47). Hence, reliable equations showing the functional relationships between radius of the CEP, turning radius, wind velocity, and horizontal system velocity may be formulated (Eq's 49 and 50) which are suitable to mission and design analysis. From the empirical relationship, we see that increased glide ratio, or horizontal system velocity,has the effect of decreasing the radius of the CEP while also decreasing the wind distortion during the approach.

APPENDIX

Glossary of Symbols and Abbreviations

a	Positive or negative unity based on homing test.
b	Value of P at R/r = 0 as determined by Method of Least Squares.
CEP	Abbreviation for circle of equal probability with center at the target.
CW	Initial position crosswind of target.
DW	Initial position downwind of target.
$\bar{h}$	Median altitude at first pass over target
h_o	Nominal deployment altitude
Δh	Error in deployment altitude.
L	Net downwind displacement during orbit measured from the ordinates of the most upwind position and the most downwind position.
ℓ_o	Nominal range at deployment
	Error in range at deployment.
ℓ/d	Glide ratio equal to ratio of range to altitude loss and also equal to ratio of lift to drag and horizontal to vertical velocity components.
m	Slope of curve for P vs R/r as determined by Method of Least Squares.
P	Probability of impact within circle of radius R.
R	Radius of circle with center at target, also referred to as distance from target.
R_c	Radius of the CEP.
r	Turning radius of the system, considered a constant by design.
S	Square of distance from target to end of arc θ.
T	Time elapsed during a typical orbit in a wind.

T_o	Time elapsed during a complete 360-degree turn in calm air.
t	Elapsed time at any position during an orbit.
UW	Initial position upwind of target.
V	Horizontal component of system velocity relative
V_d	Vertical component of system velocity relative to air, also referred to as rate of descent.
V_x	Component of V parallel to x-axis.
V_y	Component of V parallel to y-axis.
W	Wind velocity directed toward the target along the positive y-axis.
ΔW	Random gust velocity.
x	Displacement along the x-axis which is in the crosswind direction.
y	Displacement along the y-axis which is in the upwind direction.
α	Angle between V and pure crosswind resultant of V + W at most upwind position on orbit.
θ	Angle of arc during a turn.
ϕ	Inclination of V from the x-axis.
τ	Increment of time elapsed during turn through arc θ, also referred to as time lag.
$(\ )'$	Superscript denoting value at end of arc θ.
$(\ )_1$ or $(\ )_2$	Subscripts denoting value at one of two possible end points of arc θ resulting from homing control.
$(\overline{\ })_W$	Average at various initial positions.
$(\overline{\ })_\tau$	Average for various values of time increment.

Table 1. Input Parameters for Sample Cases

Case	V	r	τ	T_o	Pos	W
1	40	100	0.6	15.7	UW	25
2	40	100	0.6	15.7	CW	25
3	40	100	0.6	15.7	DW	25
4	40	100	1.2	15.7	UW	25
5	40	100	1.2	15.7	CW	25
6	40	100	1.2	15.7	DW	25
7	40	100	2.4	15.7	UW	25
8	40	100	2.4	15.7	CW	25
9	40	100	2.4	15.7	DW	25
10	60	100	0.42	10.5	UW	25
11	60	100	0.84	10.5	UW	25
12	60	100	1.68	10.5	UW	25
13	40	75	0.47	11.8	UW	25
14	40	75	0.95	11.8	UW	25
15	40	75	1.90	11.8	UW	25
16	60	75	0.31	7.85	UW	25
17	60	75	0.63	7.85	UW	25
18	60	75	1.26	7.85	UW	25
19	40	100	0.6	15.7	OT	4
20	40	100	0.6	15.7	OT	10
21	40	100	0.6	15.7	OT	32
	(fps)	(ft)	(sec)	(sec)		(fps)

Table 2A. Comparison of Actual Computer Results with Basic Orbit Geometry

(W = 25 fps)

Conditions	V = 40 fps r = 100 ft θ = 38.6°				V = 60 fps r = 100 ft θ = 24.6°		V = 40 fps r = 75 ft θ = 38.6°		V = 60 fps r = 75 ft θ = 24.6°	
Case No	1	2	3	(calc)*	10	(calc)*	13	(calc)*	16	(calc)*
L (ft)	434	435	434	436	349	350	336	328	264	261
T (sec)	42.0	41.4	42.5	42.0	18.1	18.0	37.5	31.5	15.2	13.5
X_B (ft)	-21	-24	-37	-38	-46	-58	+31	-28	-11	-44
Y_B (ft)	51	30	29	22	70	44	+49	16	74	32
X_C (ft)	-178	-190	-195	-200	-189	-200	-86	-150	-115	-150
Y_C (ft)	-162	-185	-187	-196	-104	-130	-116	-148	-55	-98
X_D (ft)	-24	-25	-38	-38	-46	-58	+29	-28	-14	-44
Y_D (ft)	-383	-405	-405	-414	-279	-306	-287	-312	-190	-229
X_E (ft)	21	9	5	0	12	0	+64	0	35	0
Y_E (ft)	-364	-388	-385	-392	-242	-262	-274	-295	-161	-197

*Calculated by equations of Section 2a.

Table 2B, Comparison of Adjusted Computer Results with Basic Orbit Geometry

Conditions	V = 40 fps r = 100 ft θ = 38.6°				V = 60 fps r = 100 ft θ = 24.6°		V = 40 fps r = 75 ft θ = 38.6		V = 60 fps r = 75 ft θ = 24.6°	
Case No.	1	2	3	Calc	10	Calc	13	Calc	16	Calc
X_B*	-38	-38	-38	$\mp$ 38	-58	$\mp$ 58	-28	$\mp$ 28	-44	$\mp$ 44
Y_B	22	22	22	22	44	44	16	16	32	32
X_C	-195	-204	-196	$\mp$ 200	-201	$\mp$ 200	-145	$\mp$ 150	-148	$\mp$ 150
Y_C	-191	-193	-194	$\mp$ 196	-130	$\mp$ 130	-149	$\mp$ 148	-97	$\mp$ 98
X_D	-41	-39	-39	$\mp$ 38	-58	$\mp$ 58	-30	$\mp$ 28	-47	$\mp$ 44
Y_D	-41]	-413	-412	$\mp$ 414	-305	$\mp$ 306	-320	$\mp$ 312	-232	$\mp$ 229
X_E	4	-5	4	0	0	0	5	0	2	0
Y_E	-393	-396	-392	$\mp$ 392	-268	$\mp$ 262	-307	$\mp$ 295	-203	$\mp$ 197

*Data of Table 2A corrected for coincidence at Point B.

Table 3. Probability Relative to 200 Ft. Circle and Orbit Time Measured from Computer Results of Cases 1-9

Probability (%)

Pos.	τ = 0.6	τ = 1.2	τ = 2.4	$\bar{P}_W$
UW	53	55	60	56.0
CW	50	53	48	50.3
DW	49	51	57	52.3
$(\bar{P}_\tau)$	50.7	53.0	55.0	54.1**

Orbit Time (sec)

Pos.	τ = 0.6	τ = 1.2	τ = 2.4	$\bar{T}_W$
UW	42	43	67	50.7
CW	42	46	50	46.0
DW	42	44	50	45.3
(T_τ)	42.0	44.0	55.7	42.0*

Probability, First Orbit (%)

Pos.	τ = 0.6	τ = 1.2	τ = 2.4	$\bar{P}_W$
UW	69	64	100	77.7
CW	49	53	77	59.7
DW	47	53	100	66.7
(P_τ)	55.0	56.7	92.3	54.1**

Time, First Orbit (sec)

Pos.	τ = 0.6	τ = 1.2	τ = 2.4	$\bar{T}_W$
UW	23	30	34	29.0
CW	41	46	41	42.7
DW	41	46	29	38.7
DW	41	46	29	38.7
(T_τ)	35.0	40.7	34.7	42.0*

Note: $(\bar{\ })_W$ is average at various initial positions
$(\bar{\ })_\tau$ is average for various time increments
* calculated by Eq (19)
** calculated by Eq (47)

Table 4. Graphically-Determined Probability for Cases 1,10,13,16,19,20, and 21

W (fps)	4	10	25	25	25	25	32
V (fps)	40	40	60	60	40	40	40
r (ft)	100	100	75	100	75	100	100
R (ft)							
50	15%	15	23	19	25	19	18
100	33	32	46	35	41	31	29
150	48	47	66	29	54	43	39
200	85	65	84	65	72	53	48
250	100	100	100	80	85	65	57
300	100	100	100	88	94	76	66
350	100	100	100	100	100	86	75
400	100	100	100	100	100	100	85

Table 5. Graphically-Determined Probability As a Function of Dimensionless Parameters R/r and W/V for Cases 1,10,13,16,19,20 and 21

W (fps)	4	10	25	25	25	25	32
V (fps)	40	40	60	60	40	40	40
r (ft)	100	100	75	100	75	100	100
W/V	0.10	0.25	0.42	0.42	0.625	0.625	0.80
R/r							
0.5	15%	15		19		19	18
0.67			23		25		
1.00	33	32		35		31	29
1.33			46		41		
1.50	48	47		49		43	39
2.00	85	65	66	65	54	53	48
2.50	100	100		80		65	57
2.67	100	100	84		72		
3.00	100	100	100	88		76	66
3.33	100	100	100	100	85		
3.50	100	100	100	100	100	86	75
4.00	100	100	100	100	100	100	85

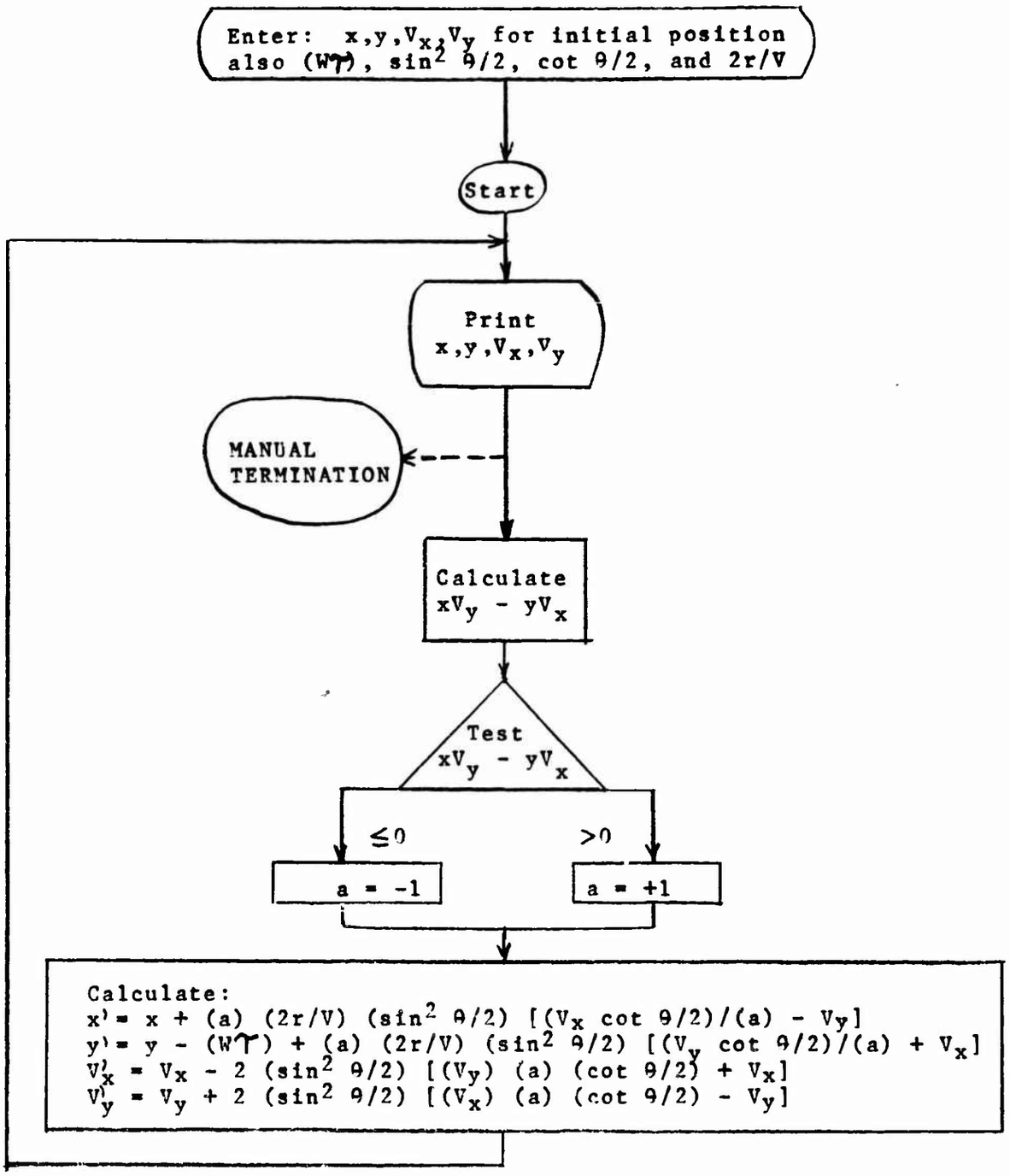

Fig 3. Flow Chart for Computer Program

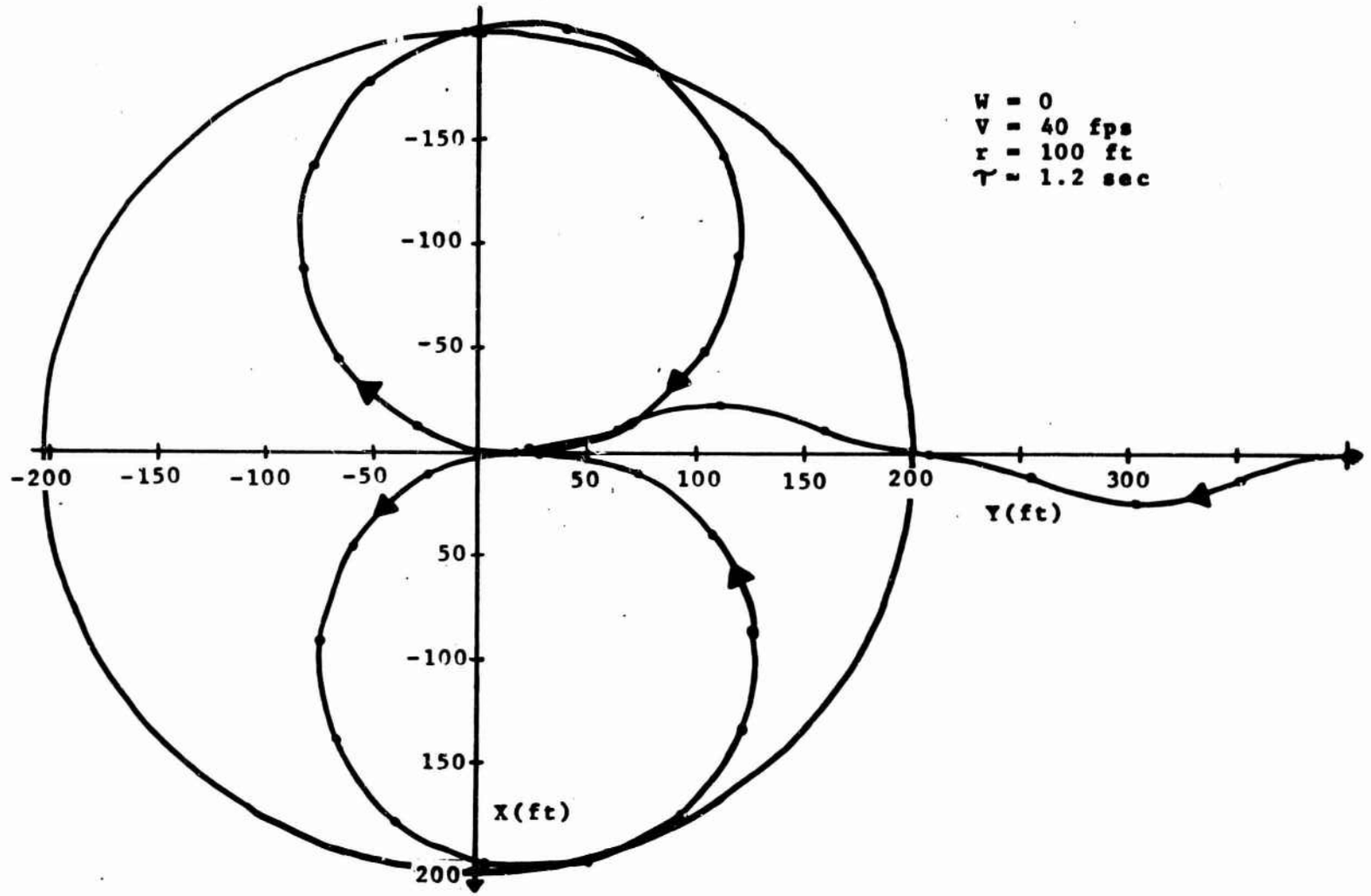

Fig 4 GROUND TRACK FOR CALM CONDITIONS

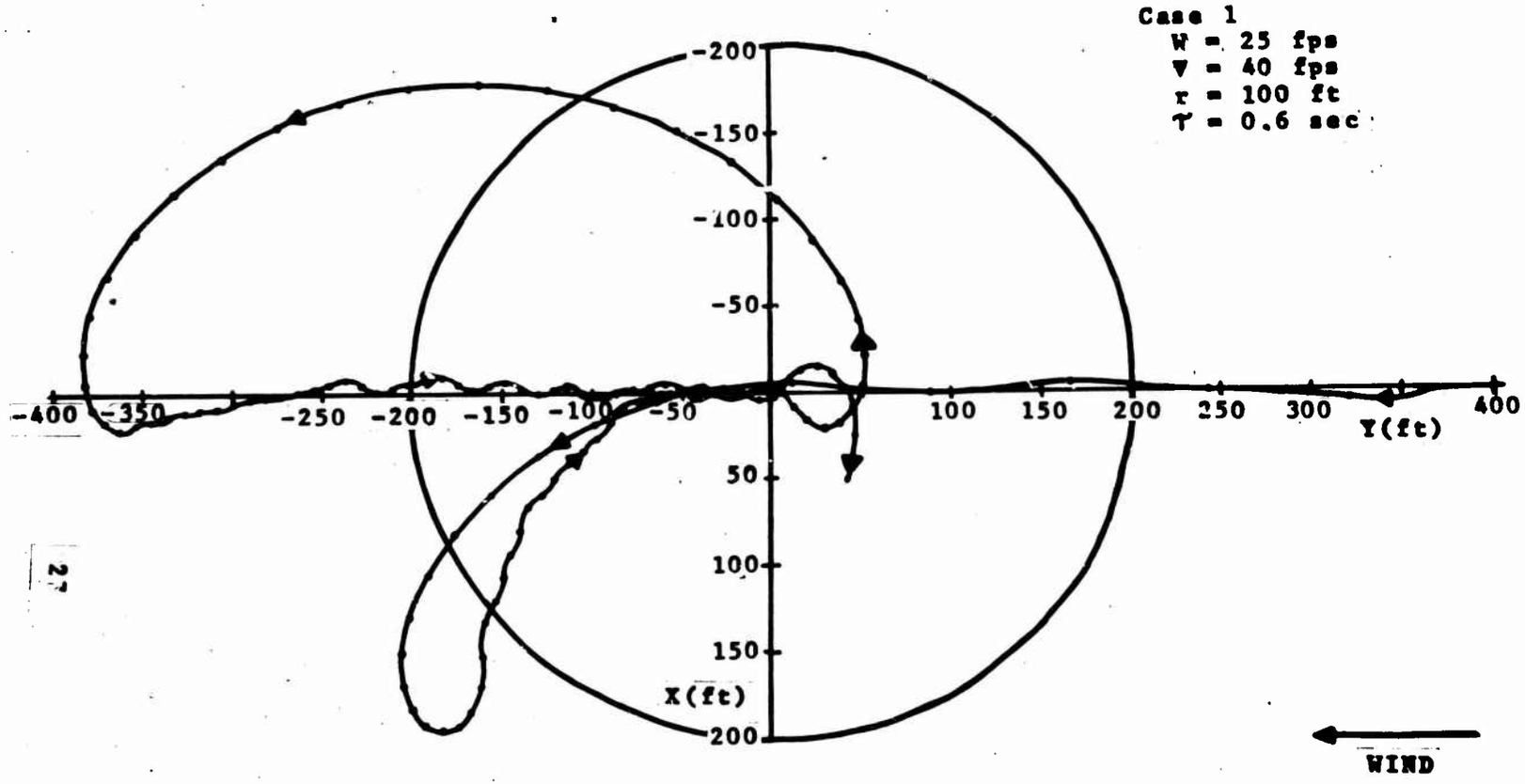

Fig 5 GROUND TRACK FOR CASE 1

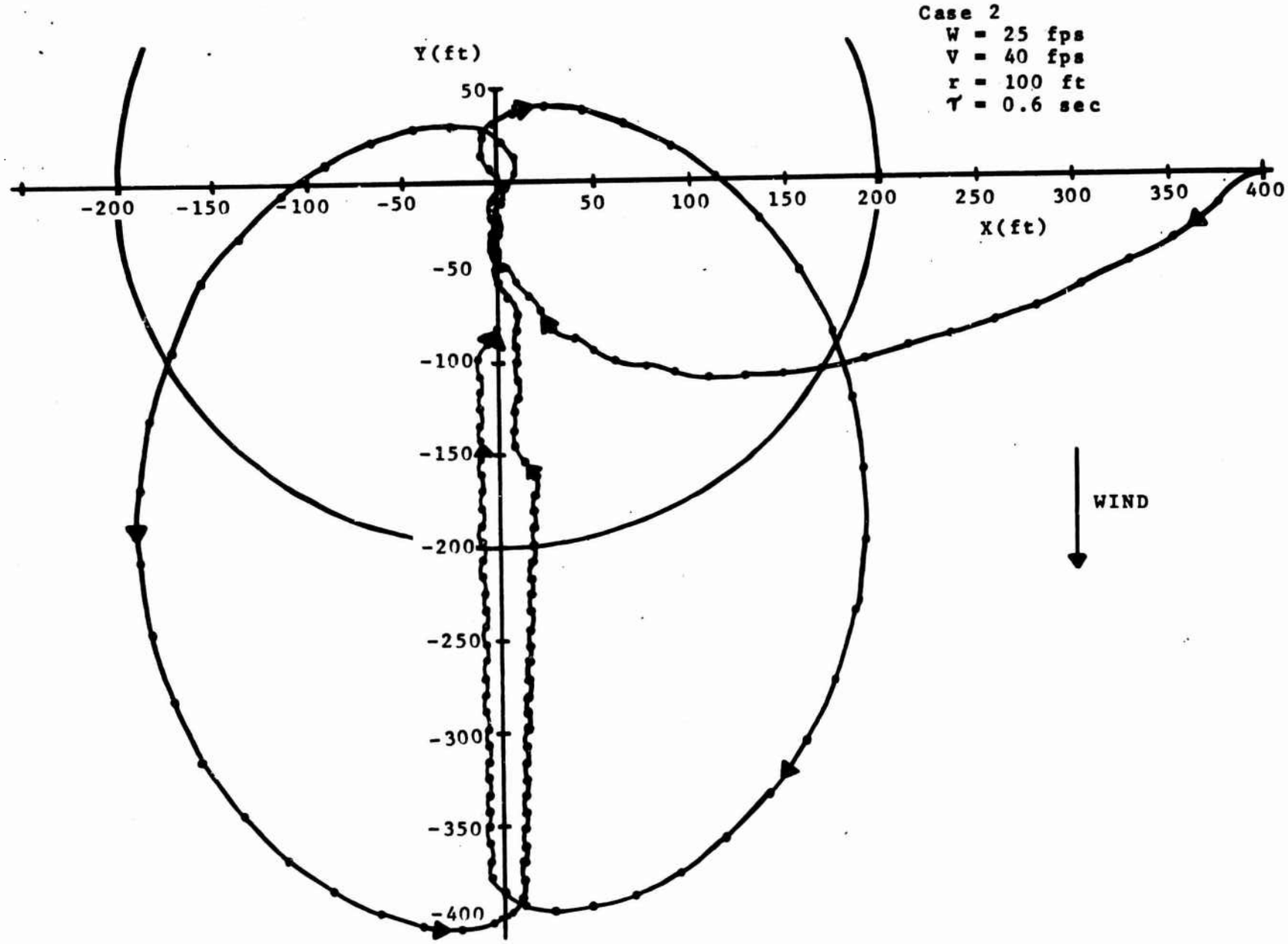

Fig 6 GROUND TRACK FOR CASE 2

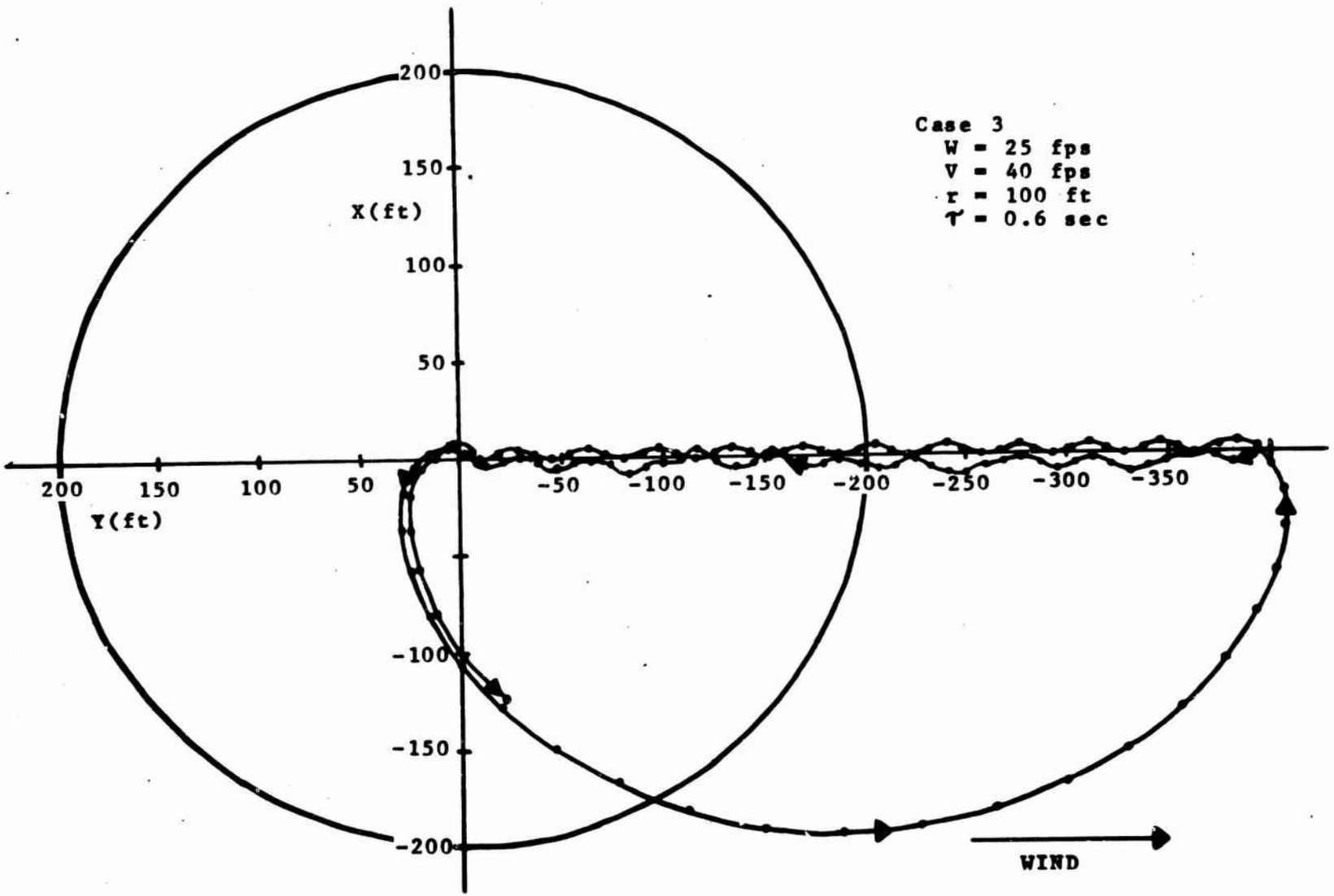

Fig 7 GROUND TRACK FOR CASE 3

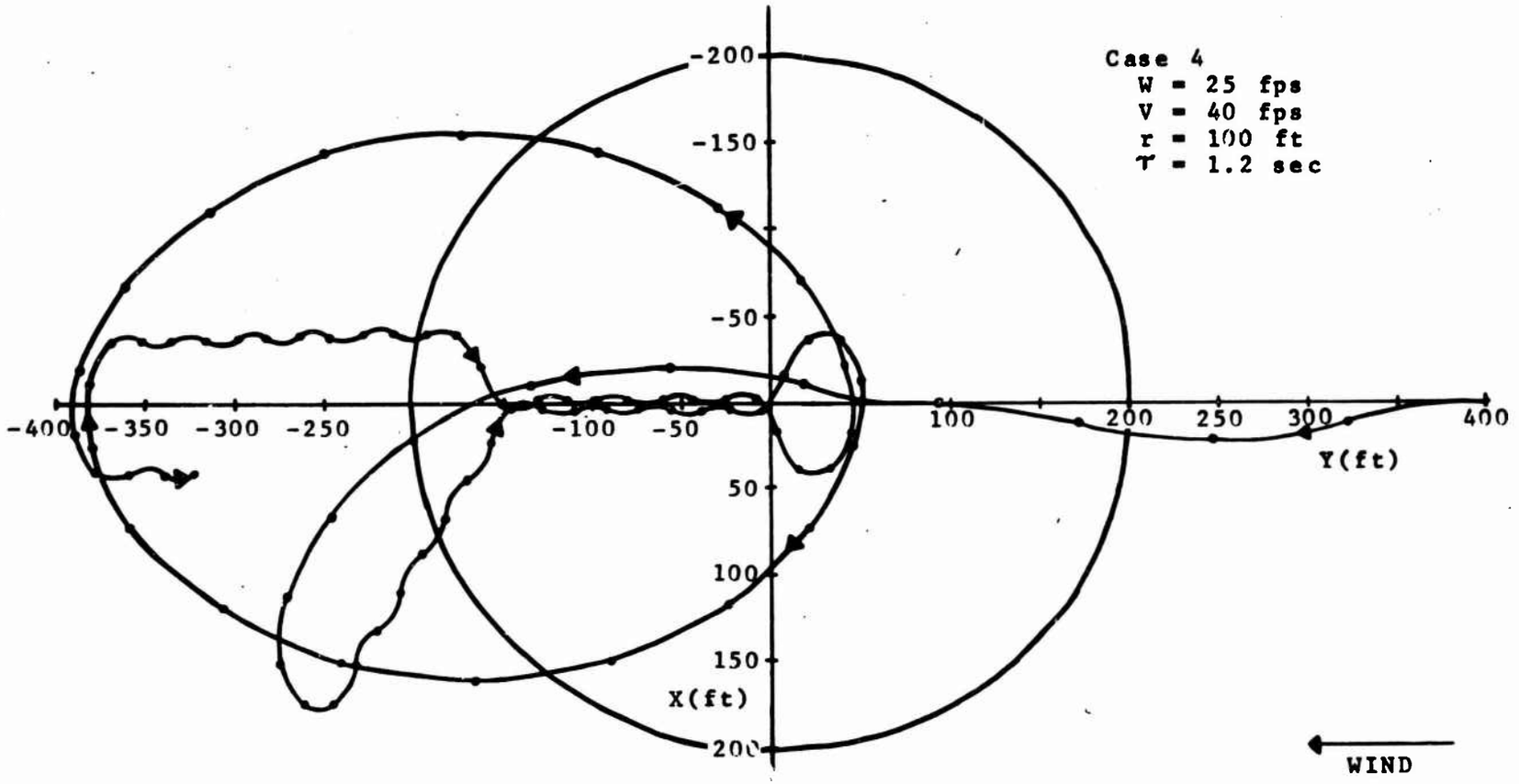

Fig 8 GROUND TRACK FOR CASE 4

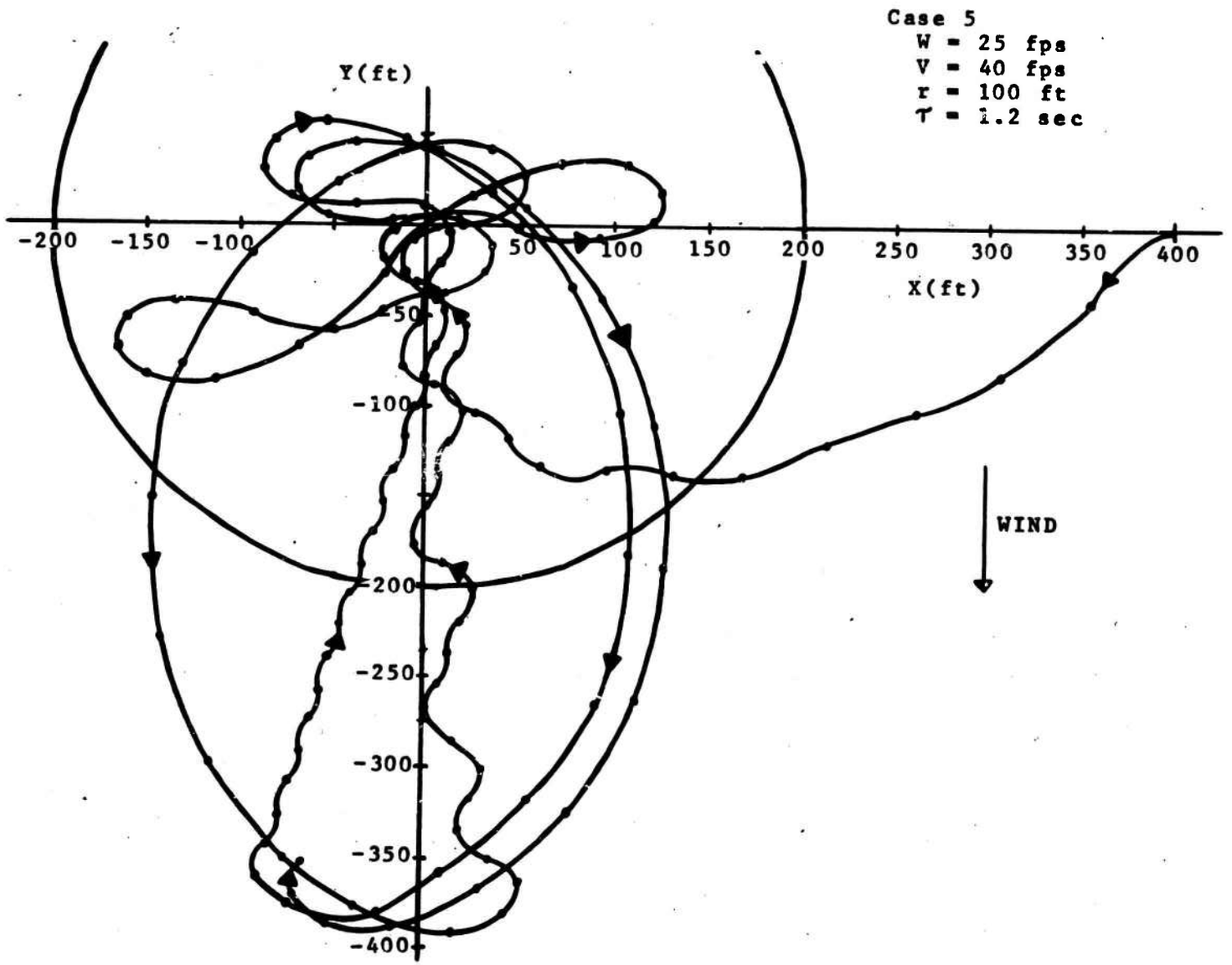

Fig 9 GROUND TRACK FOR CASE 5

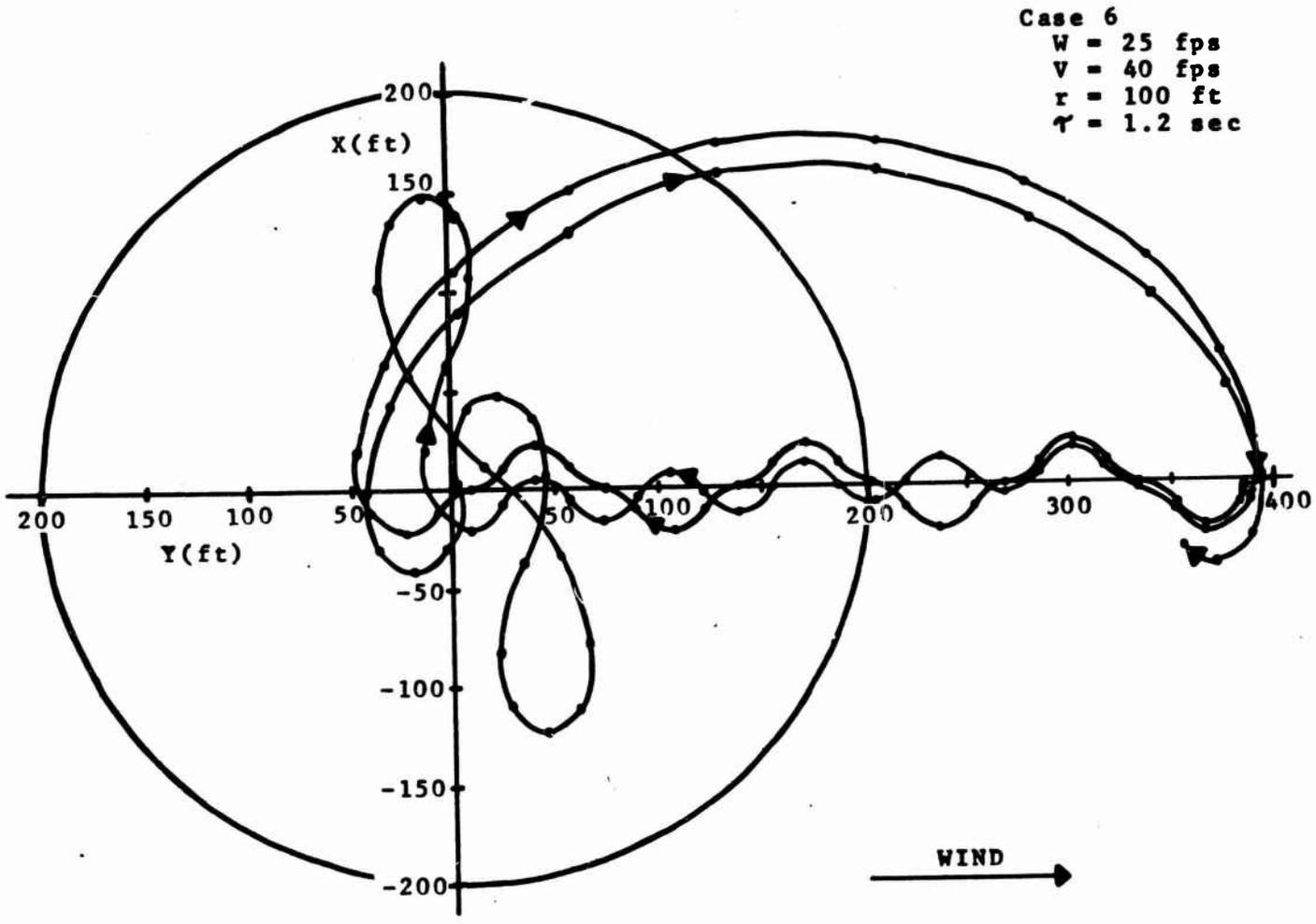

Fig 10 GROUND TRACK FOR CASE 6

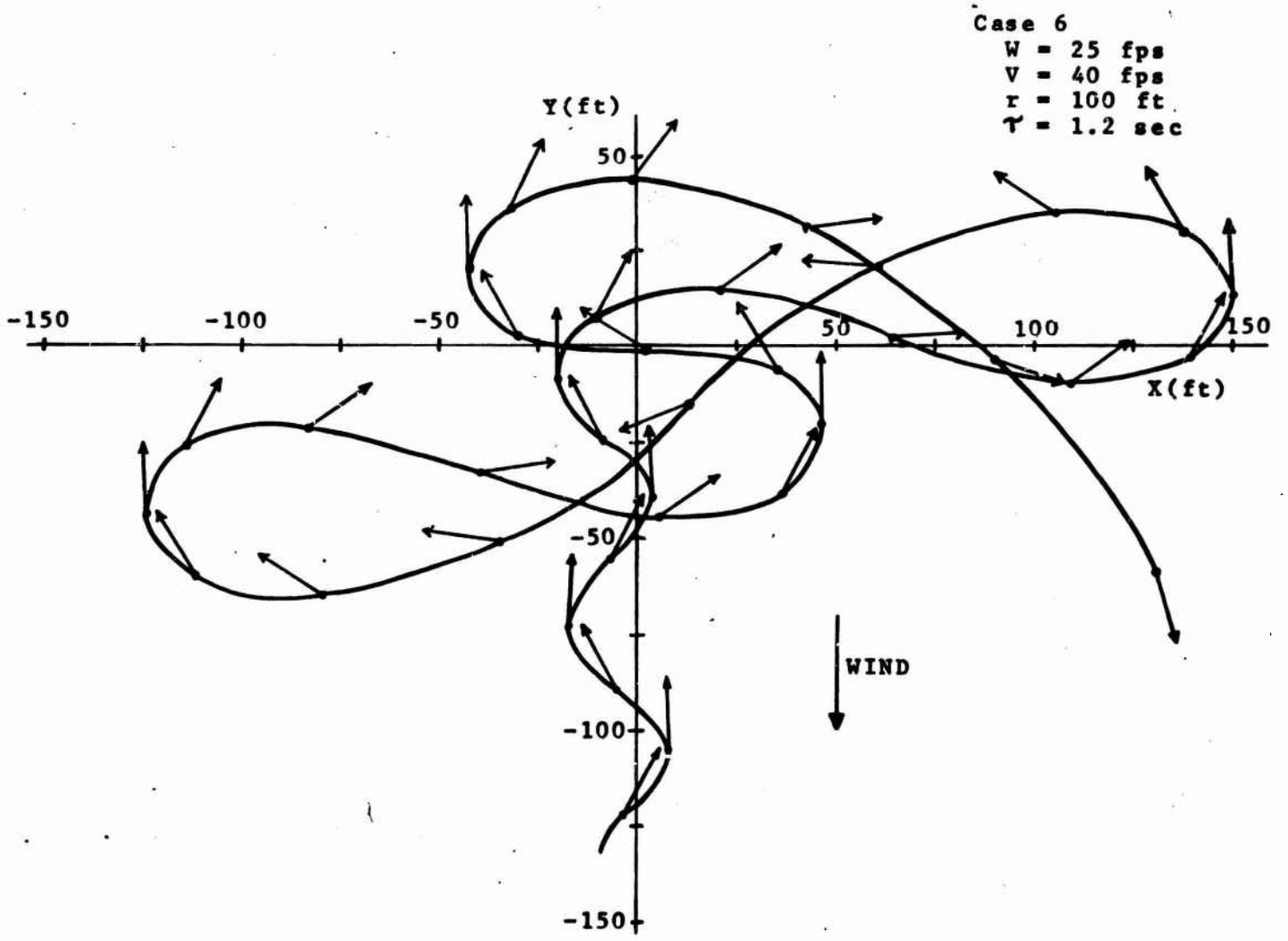

Fig 11 EXPANDED PORTION OF CASE 6 SHOWING INSTANTANEOUS SYSTEM ORIENTATIONS

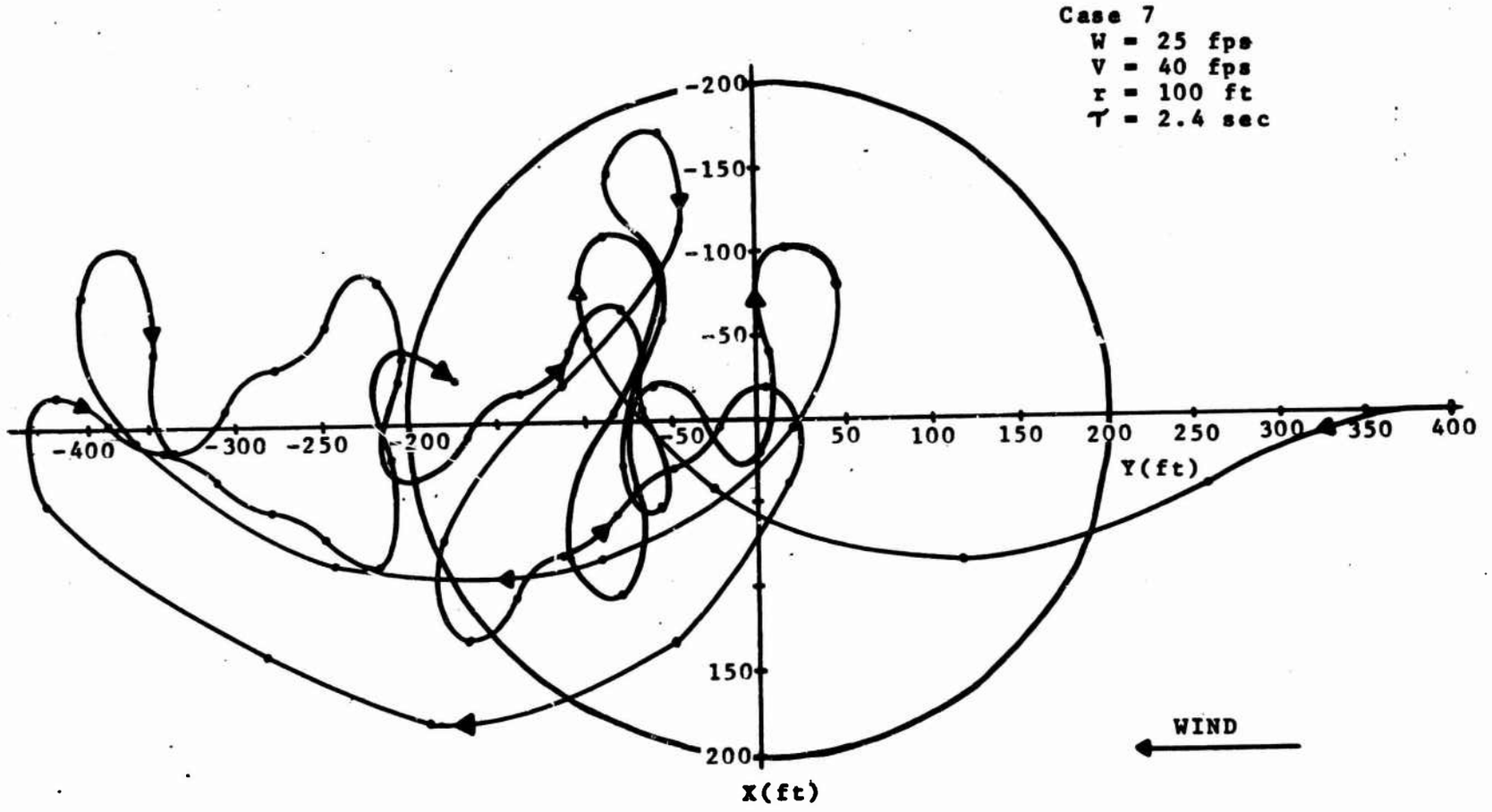

Fig 12 GROUND TRACK FOR CASE 7

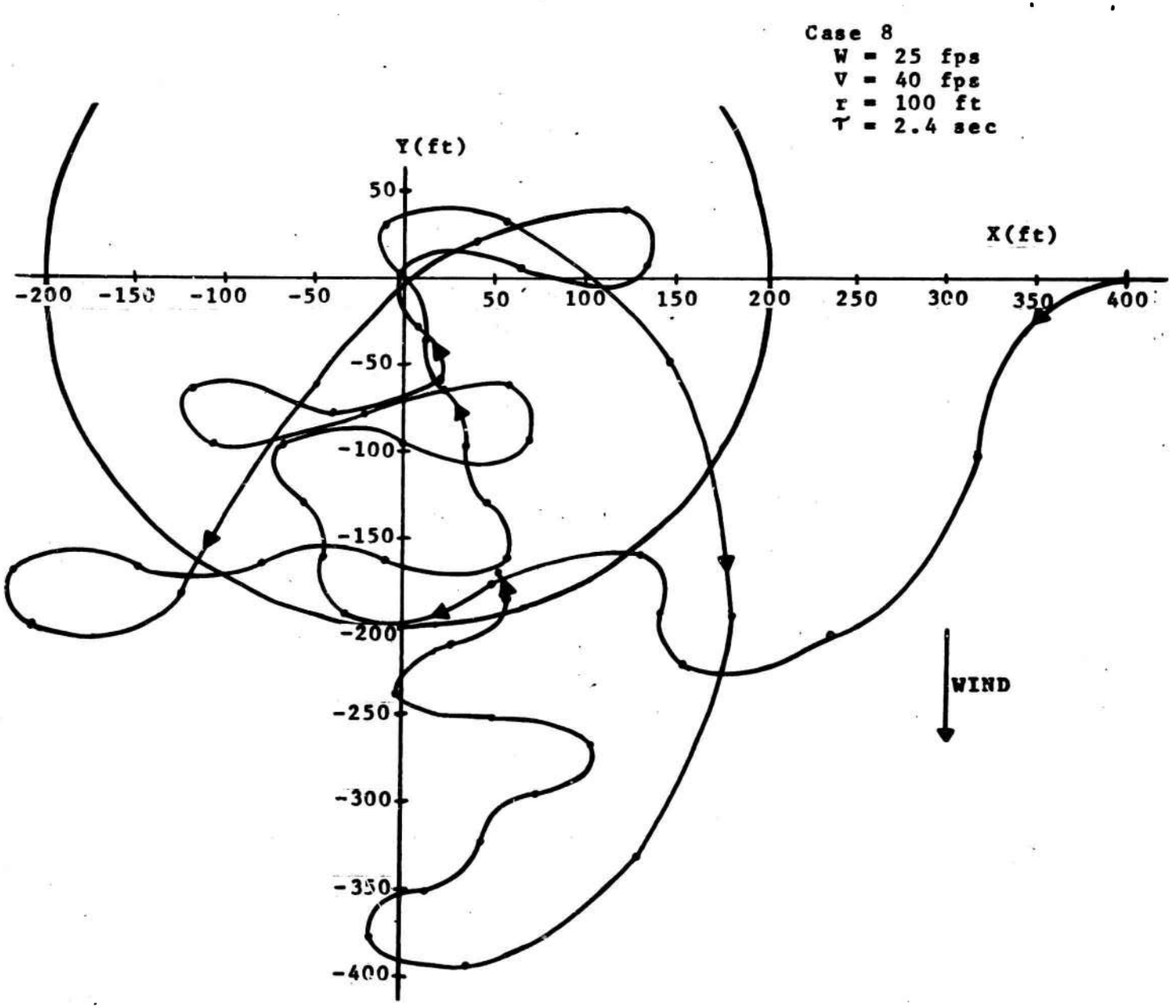

Fig 13 GROUND TRACK FOR CASE 8

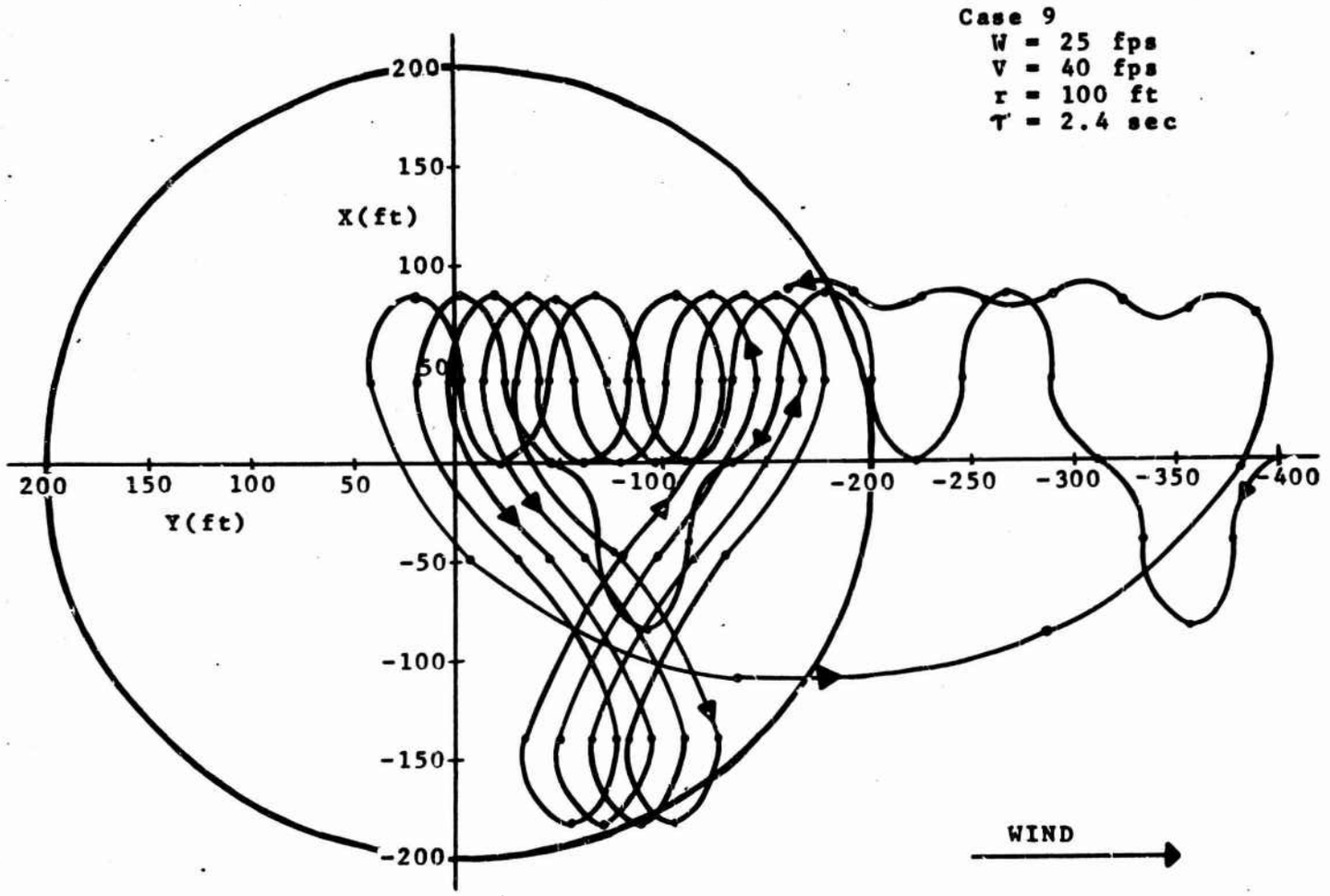

Fig 14 GROUND TRACK FOR CASE 9

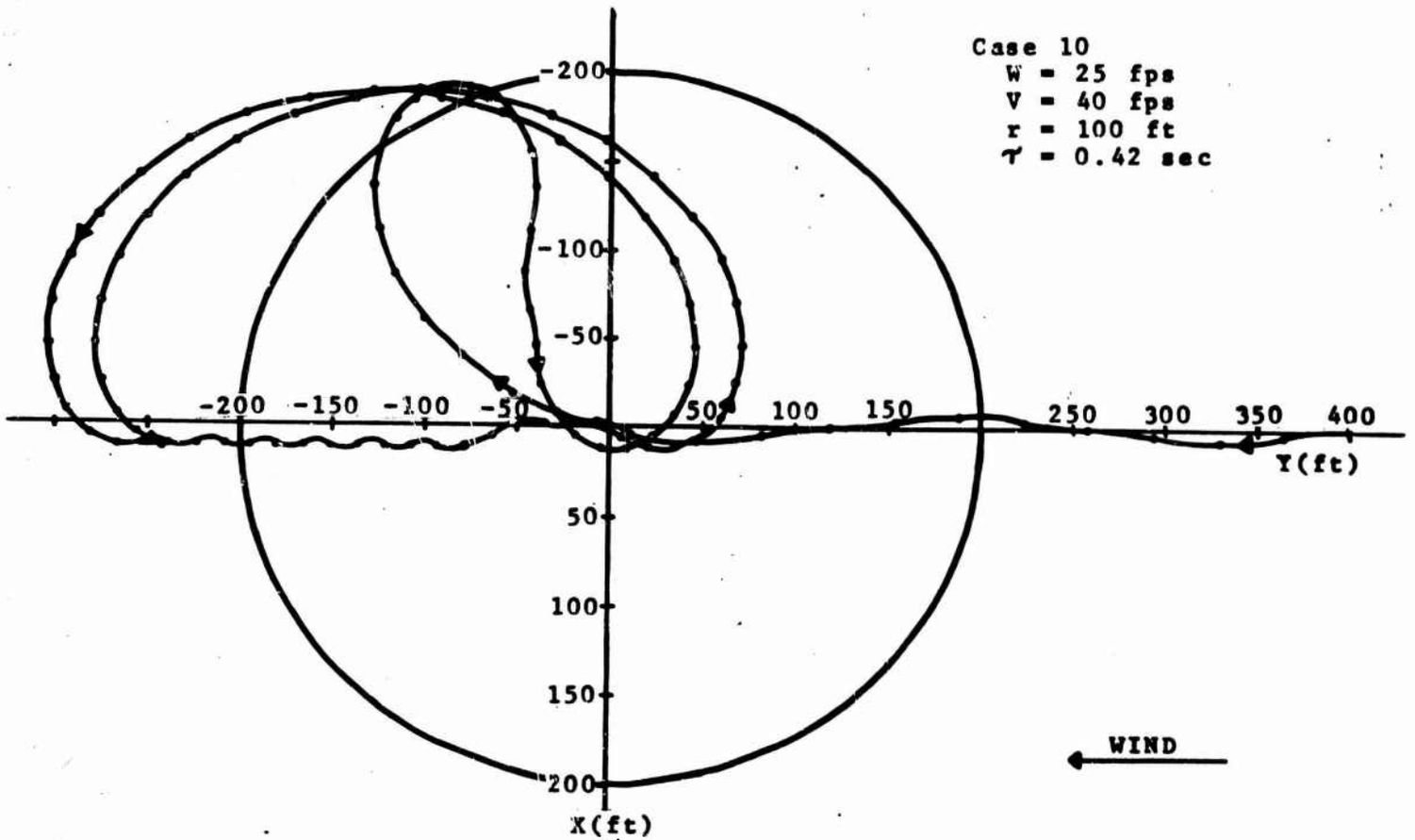

Fig 15 GROUND TRACK FOR CASE 10

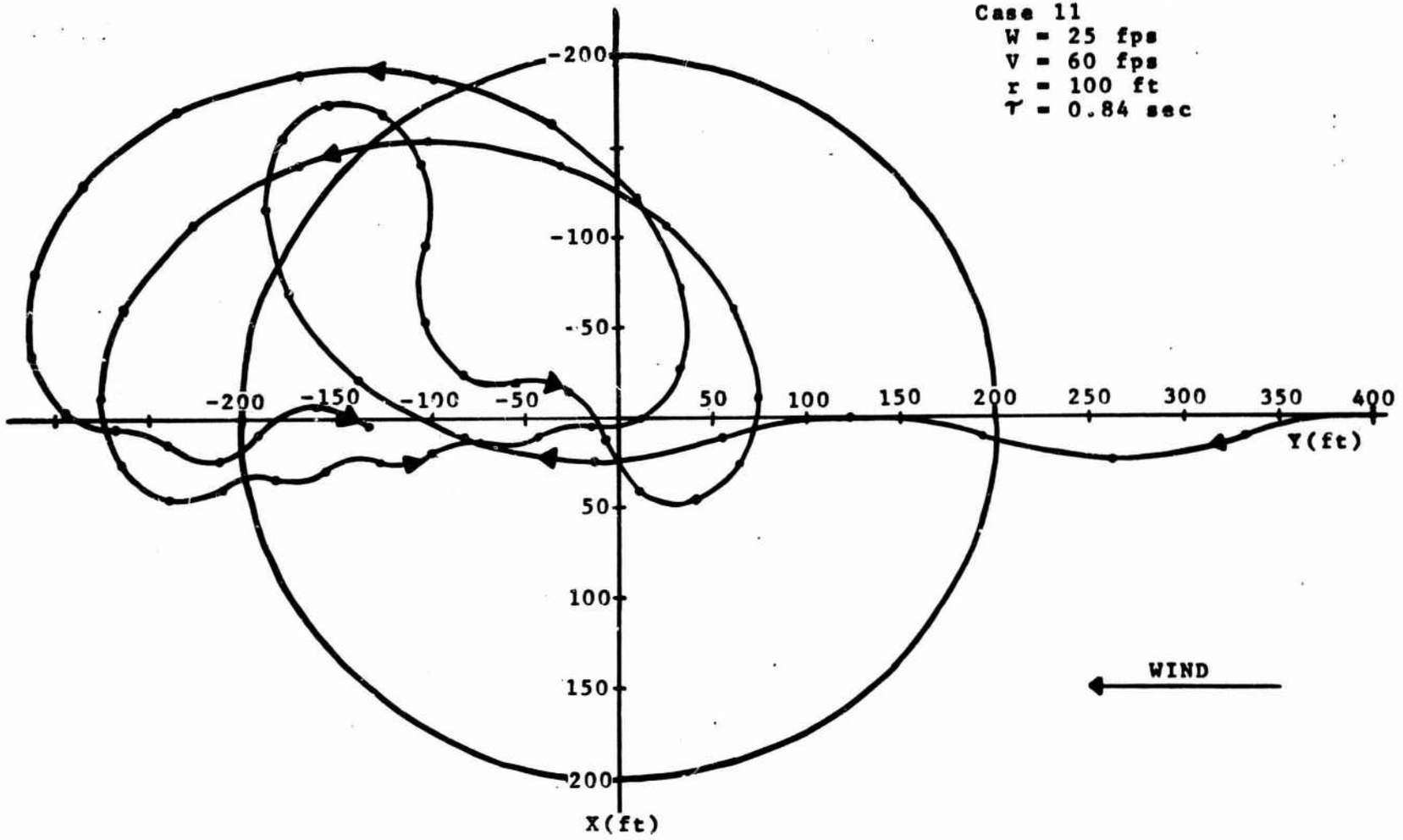

Fig 16 GROUND TRACK FOR CASE 11

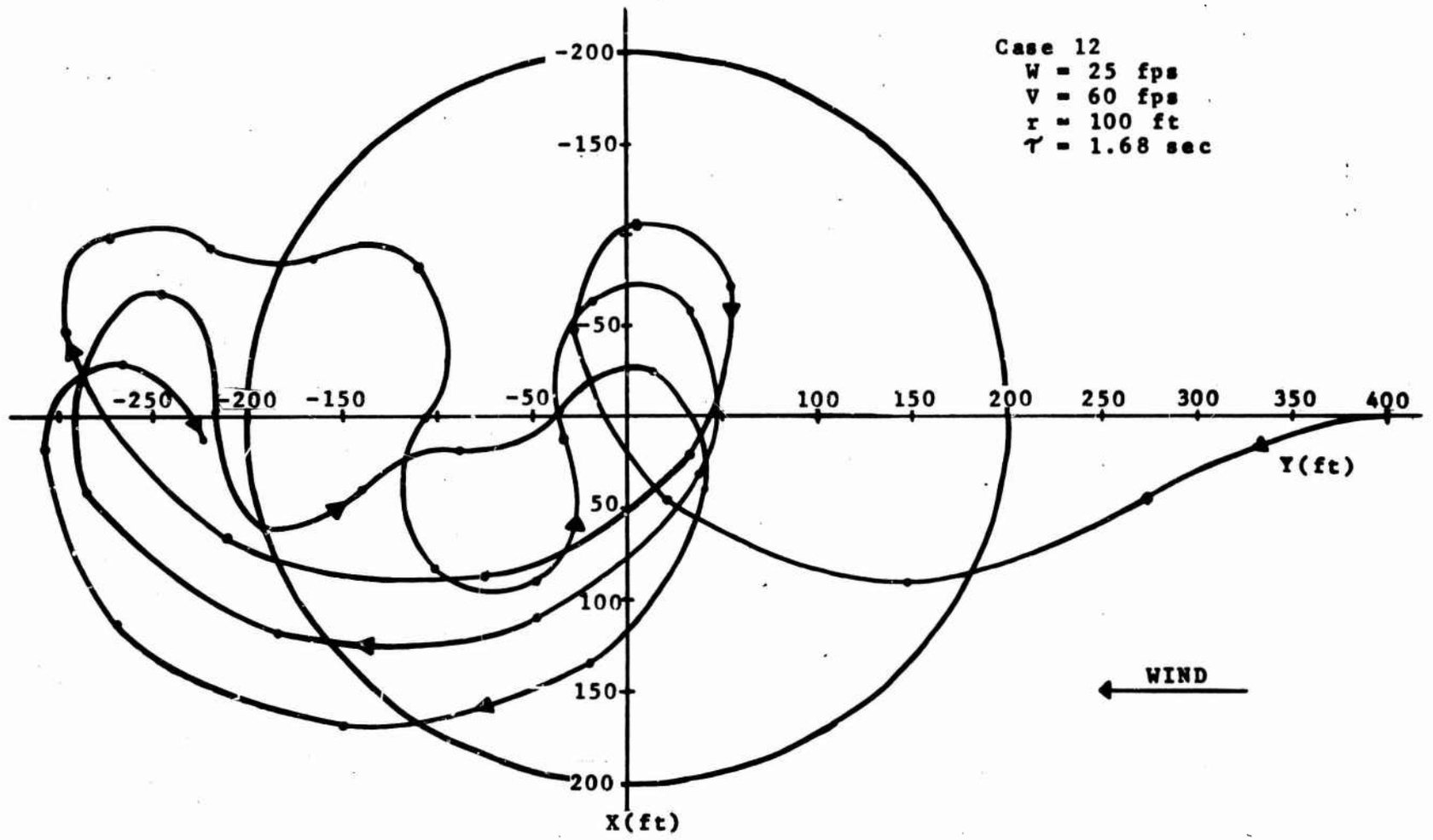

Fig 17 GROUND TRACK FOR CASE 12

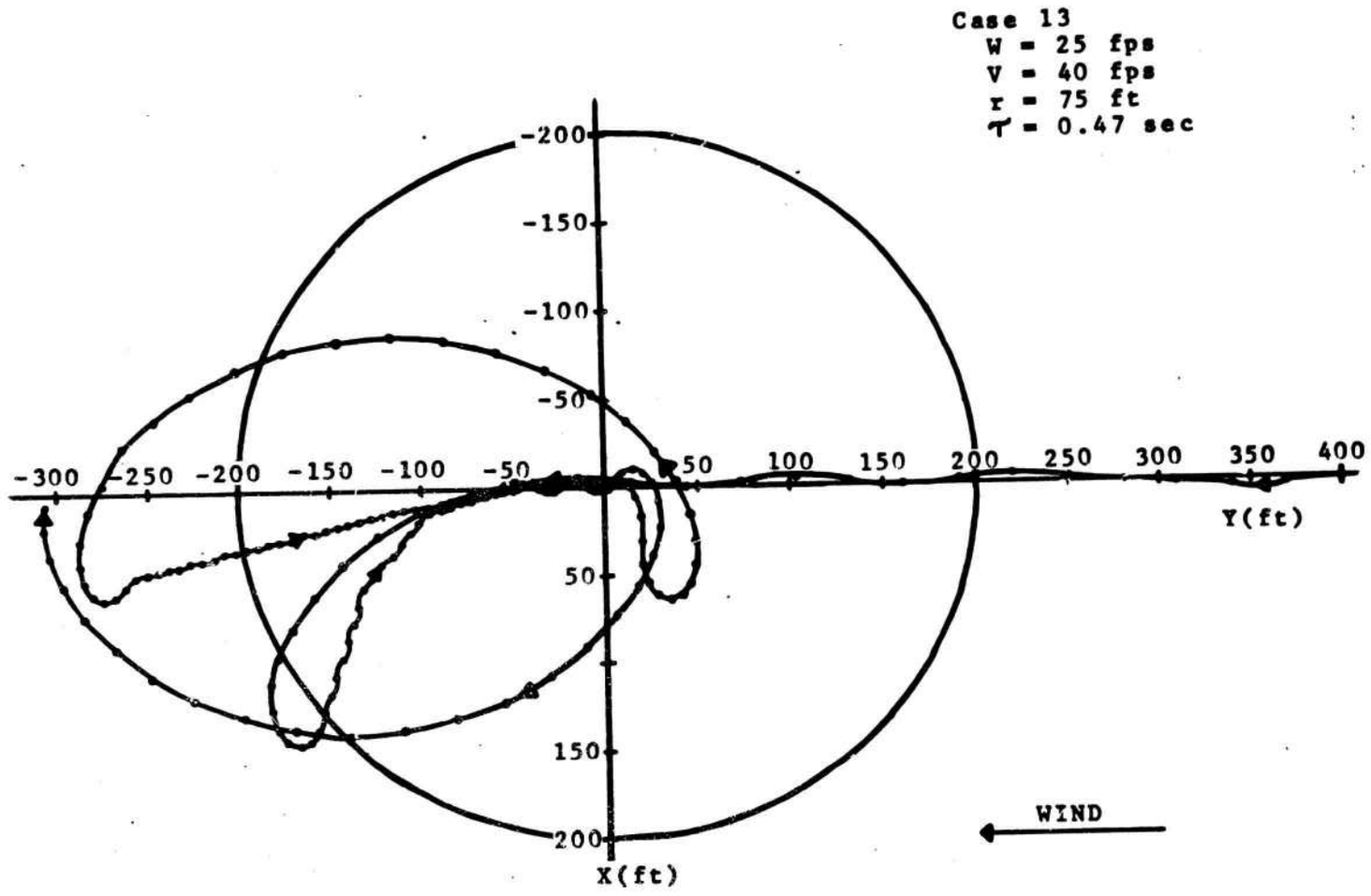

Fig 18 GROUND TRACK FOR CASE 13

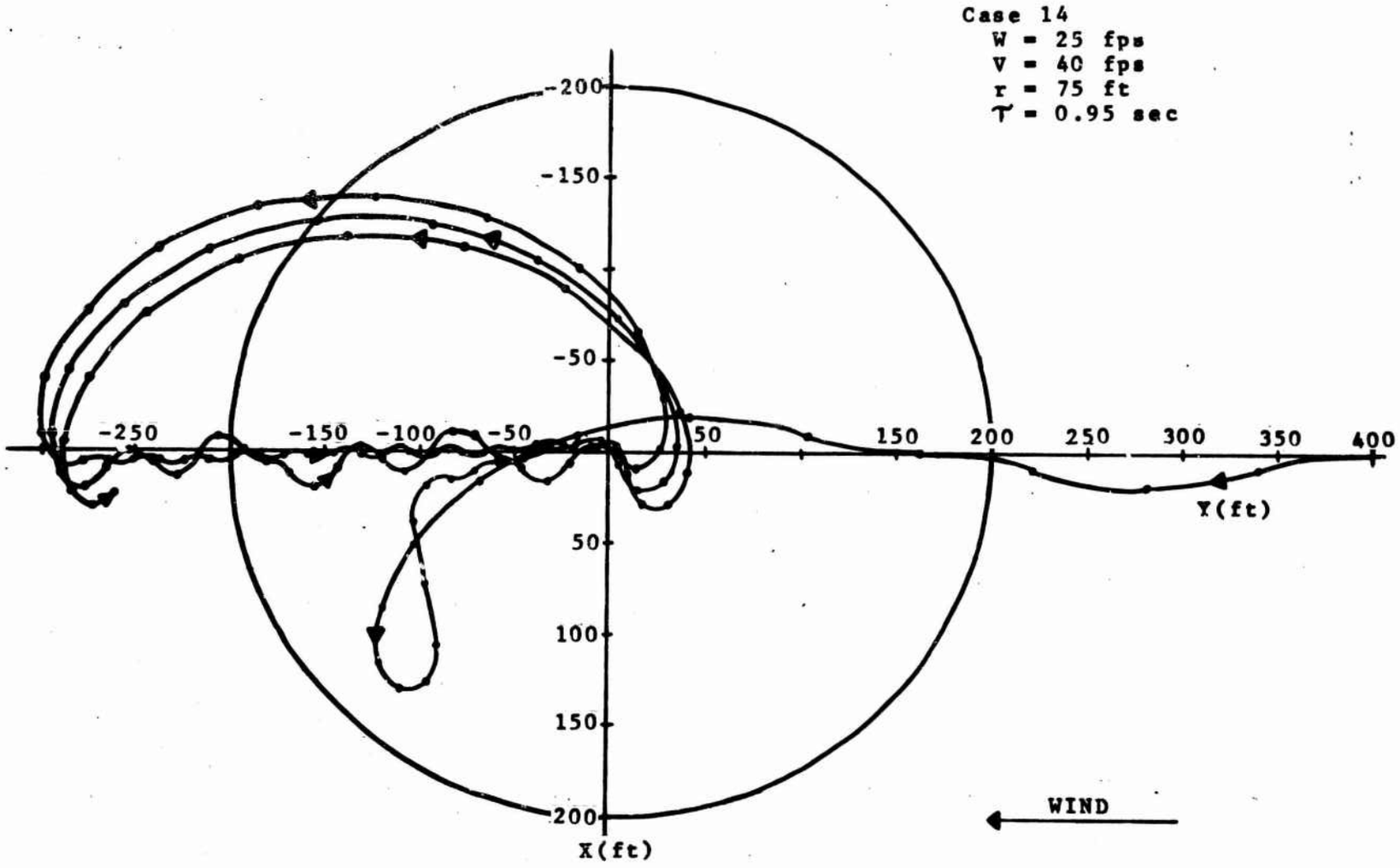

Fig 19 GROUND TRACK FOR CASE 14

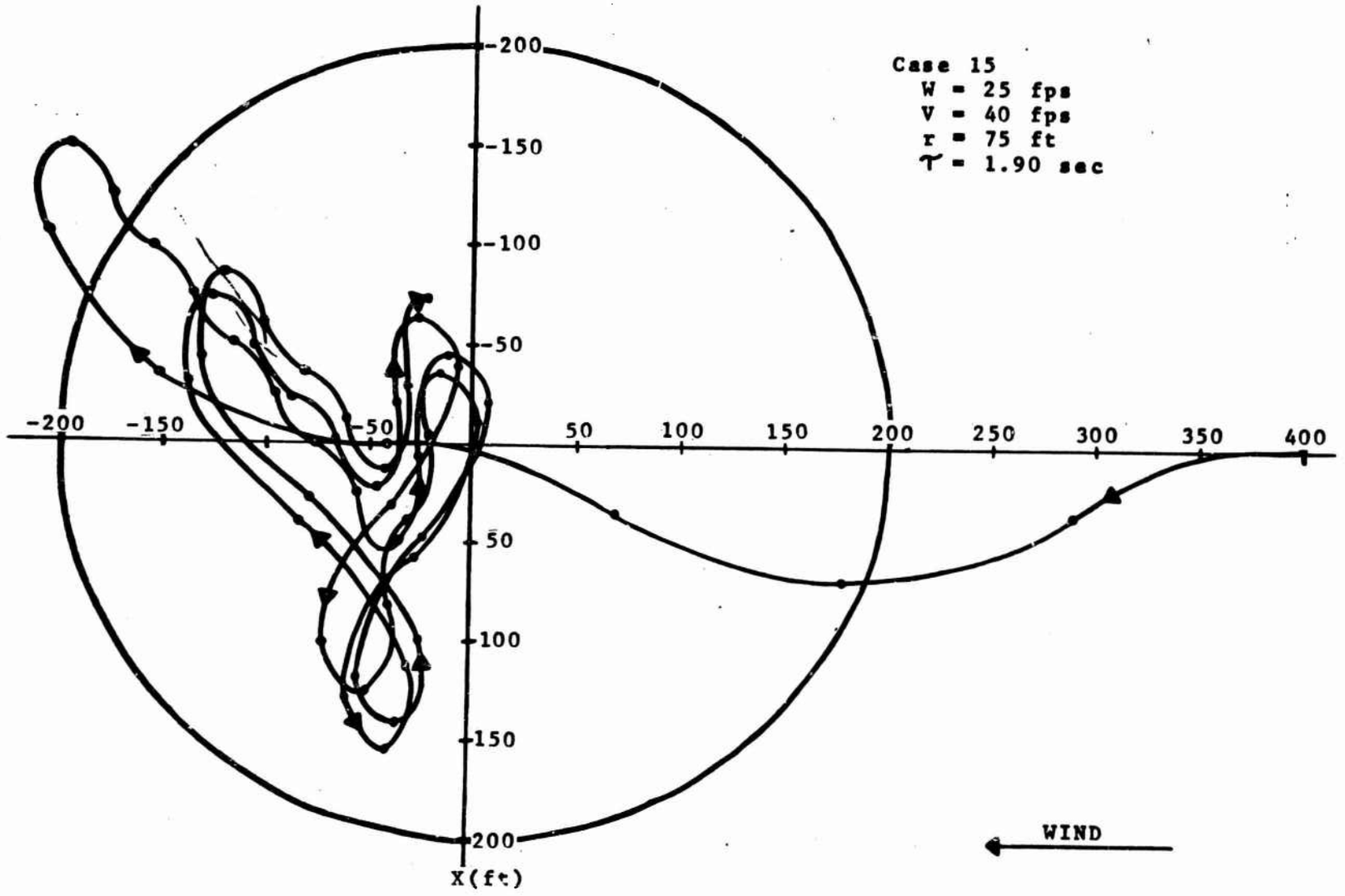

Fig 20 GROUND TRACK FOR CASE 15

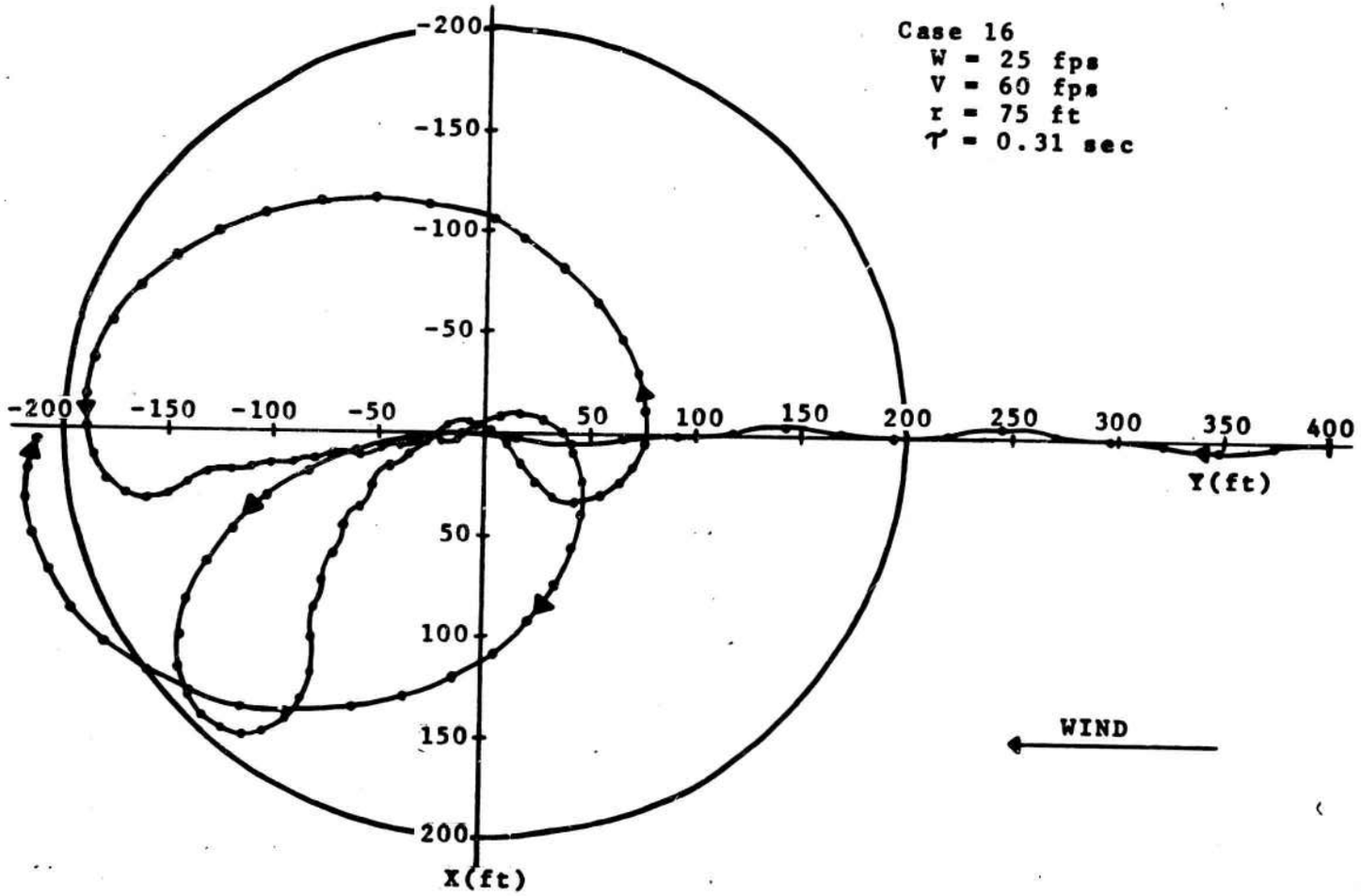

Fig 21 GROUND TRACK FOR CASE 16

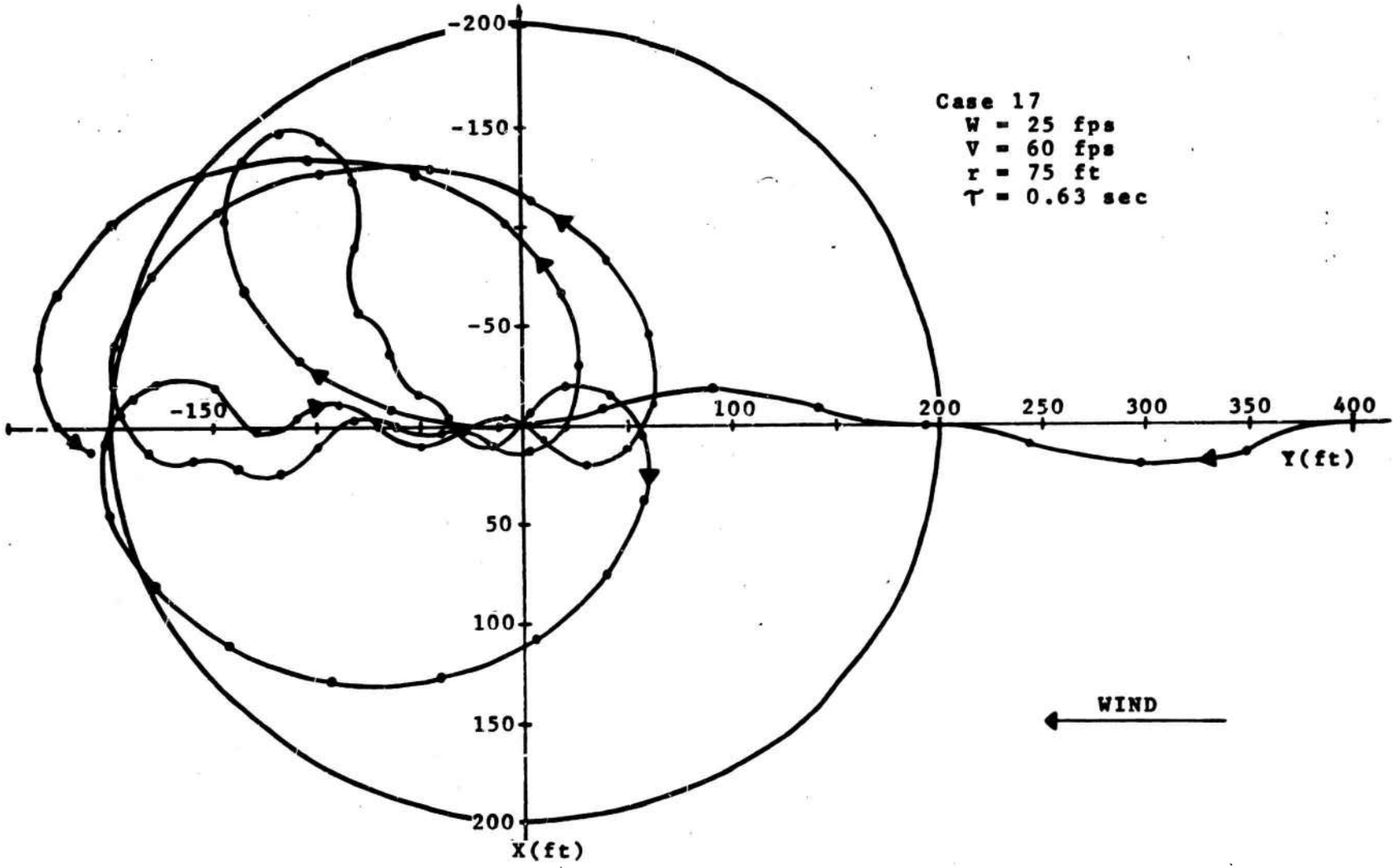

Fig 22 GROUND TRACK FOR CASE 17

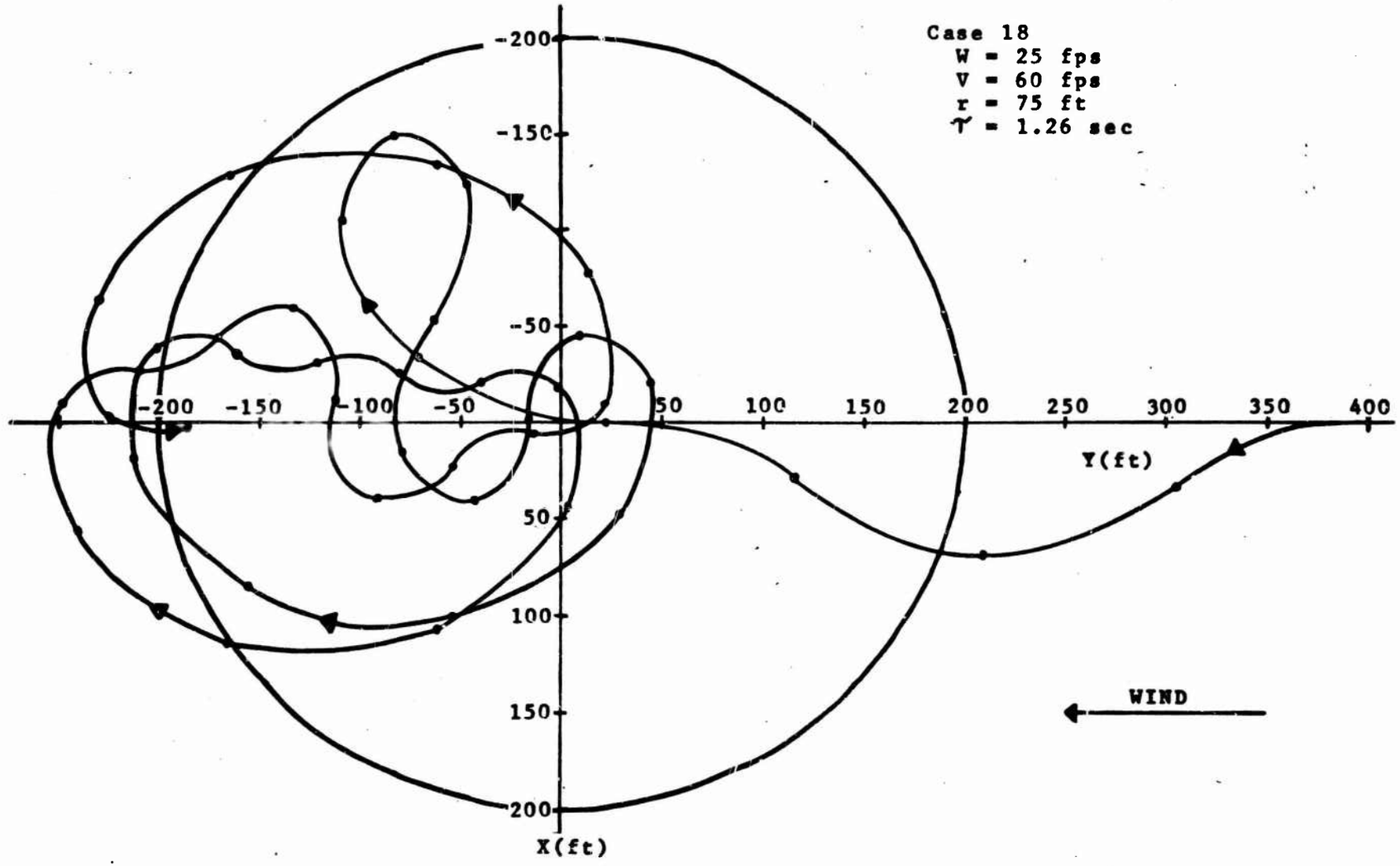

Fig 23 GROUND TRACK FOR CASE 18

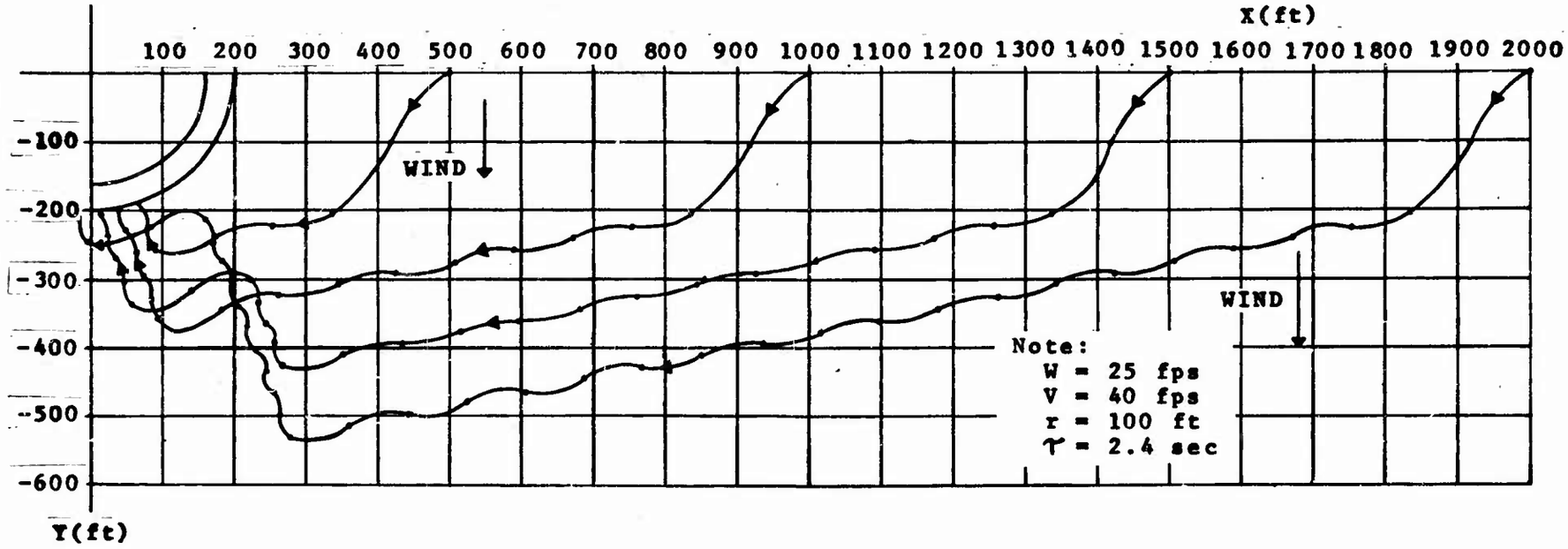

Fig 24 EFFECT OF INITIAL OFFSET ON CROSSWIND APPROACH

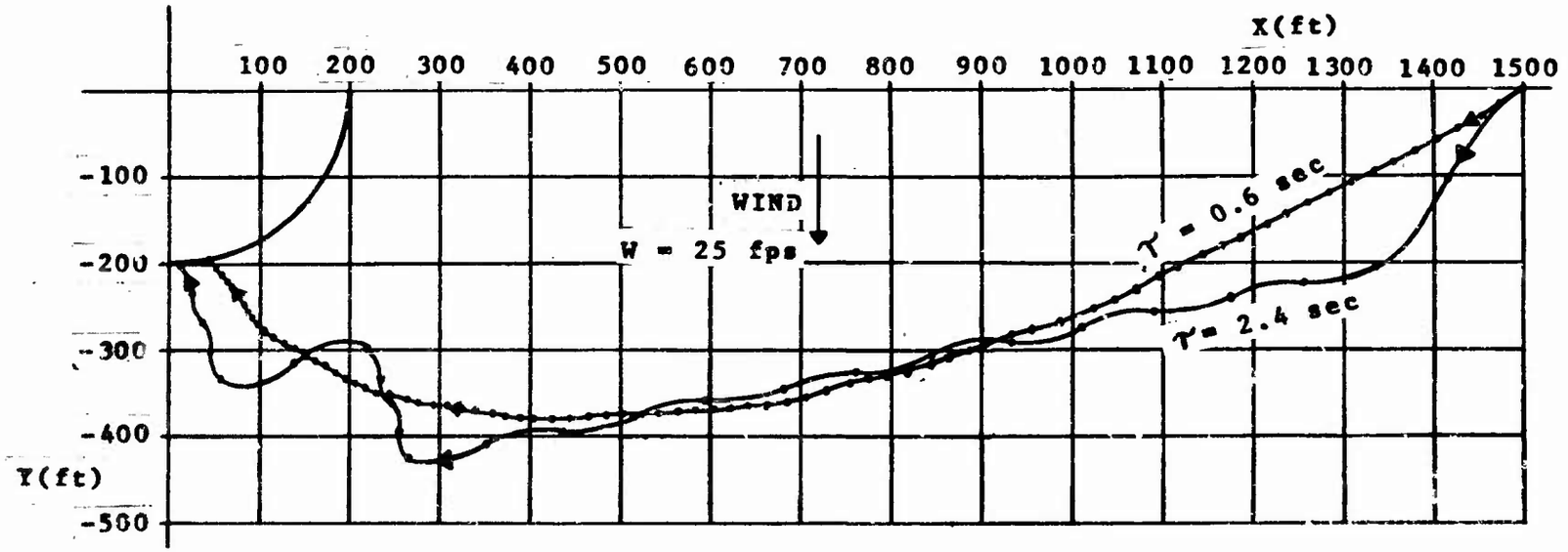

Fig 25 EFFECT OF TIME LAG ON CROSSWIND APPROACH

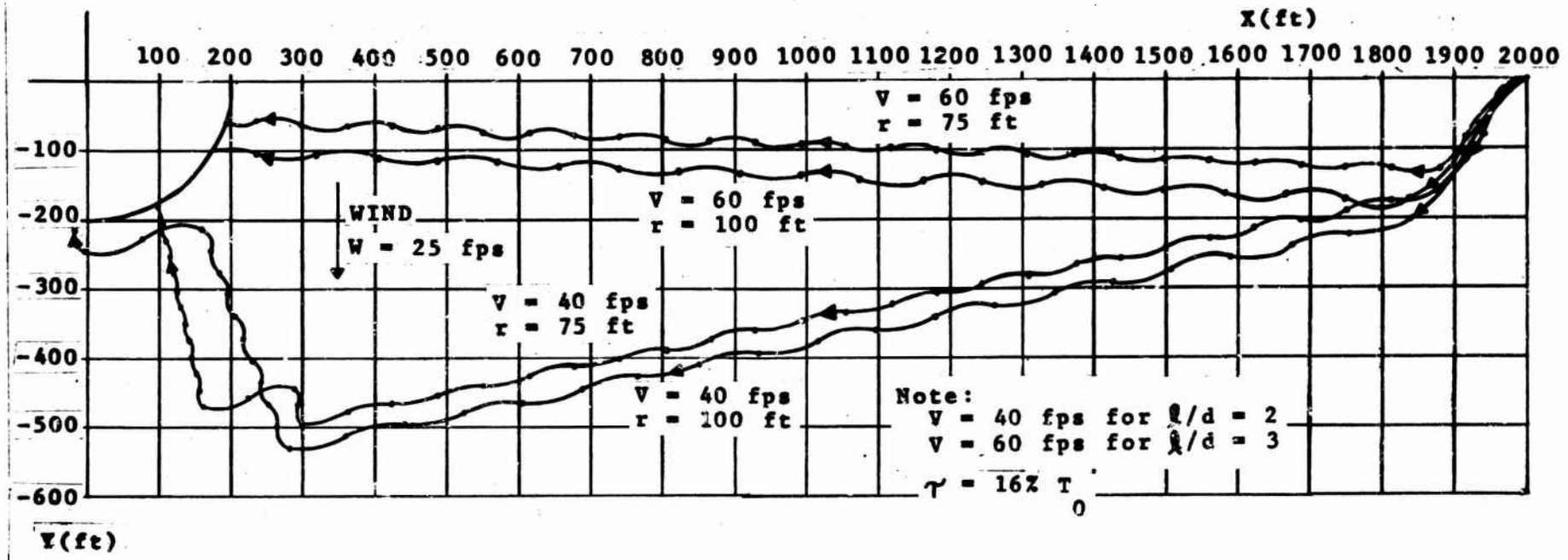

Fig 26 EFFECT OF VELOCITY AND RADIUS OF TURN ON CROSSWIND APPROACH

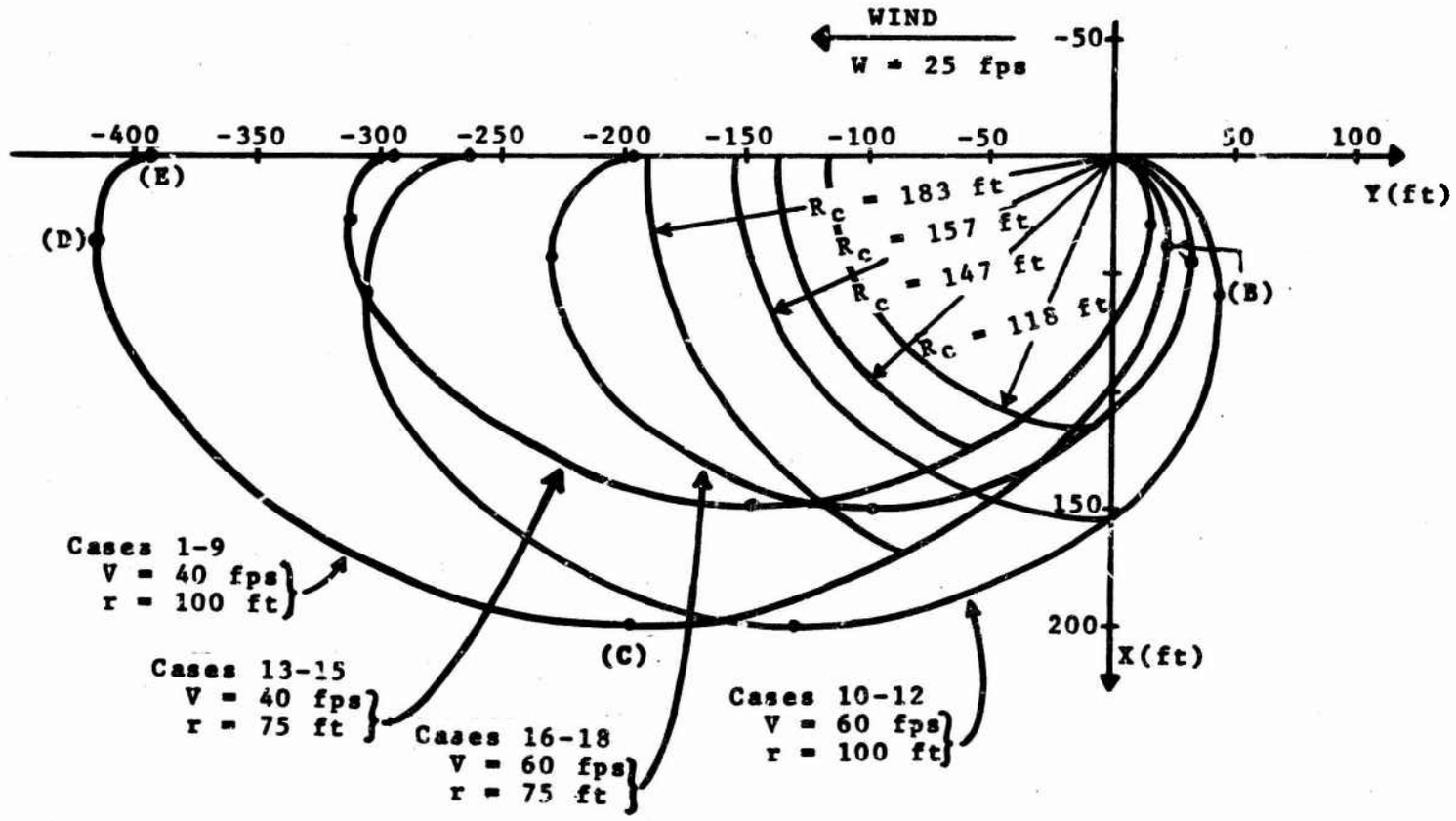

Fig 27 CHARACTERISTIC POINTS ON THEORETICAL ORBITS CORRESPONDING TO CASES 1-18

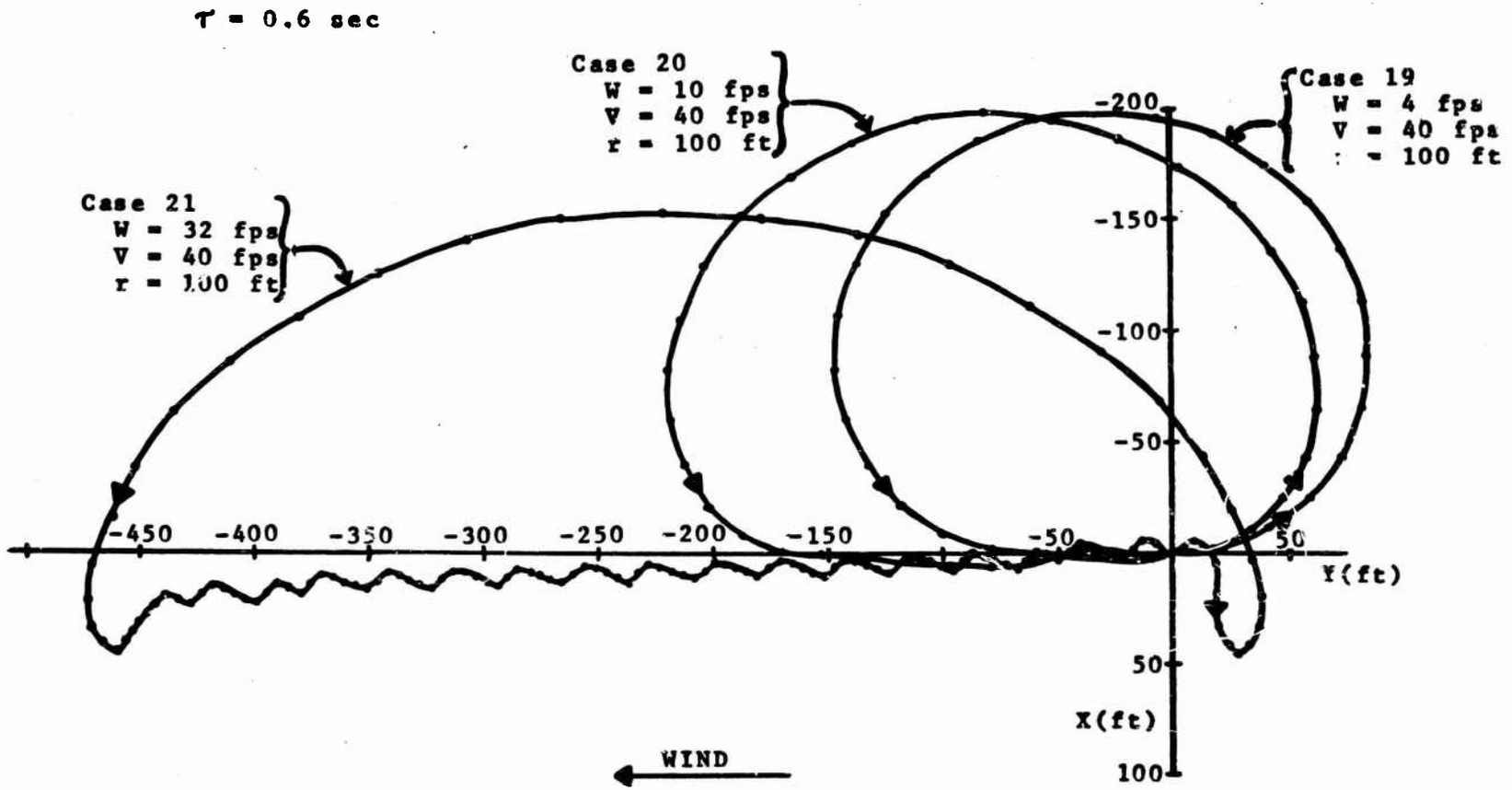

Fig 28 COMPUTED ORBITS FOR CASES 19,20,21

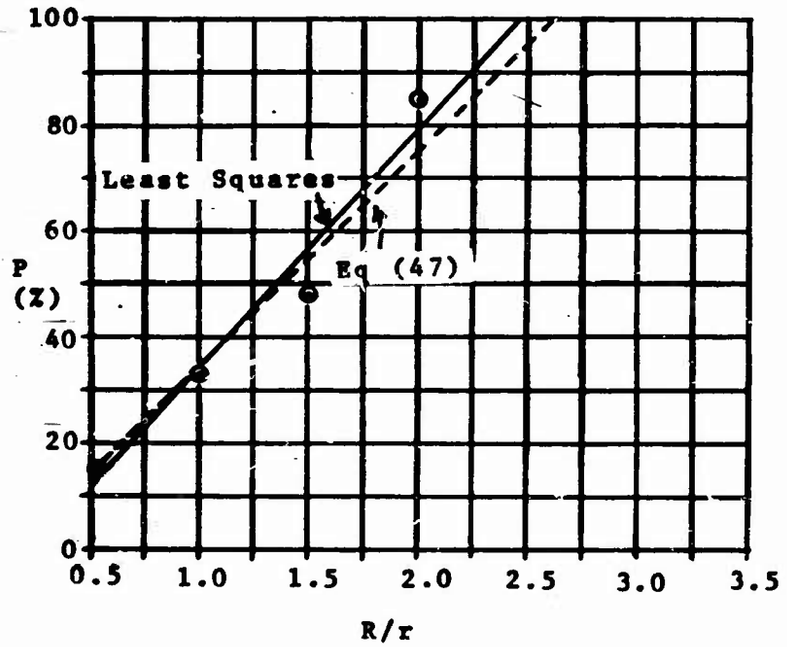

a) P vs R/r at W/V = 0.10

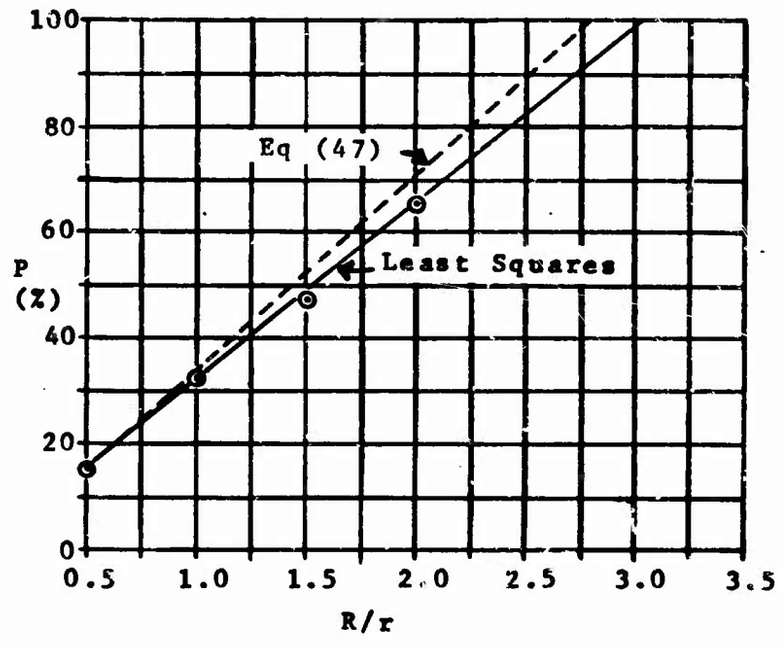

b) P vs R/r at W/V = 0.25

Fig 29 LEAST SQUARES ANALYSIS OF P vs R/r AT VARIOUS W/V

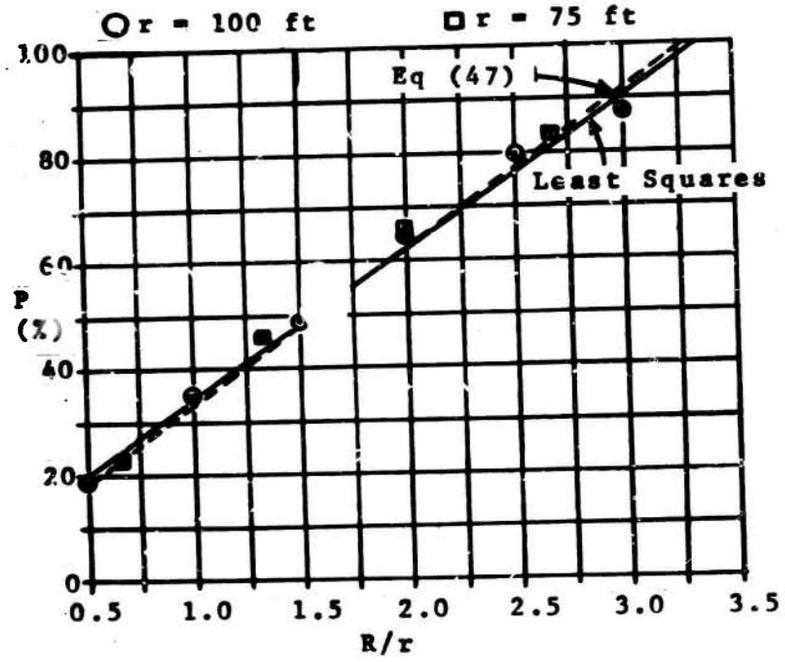

c) P vs R/r at W/V = 0.42

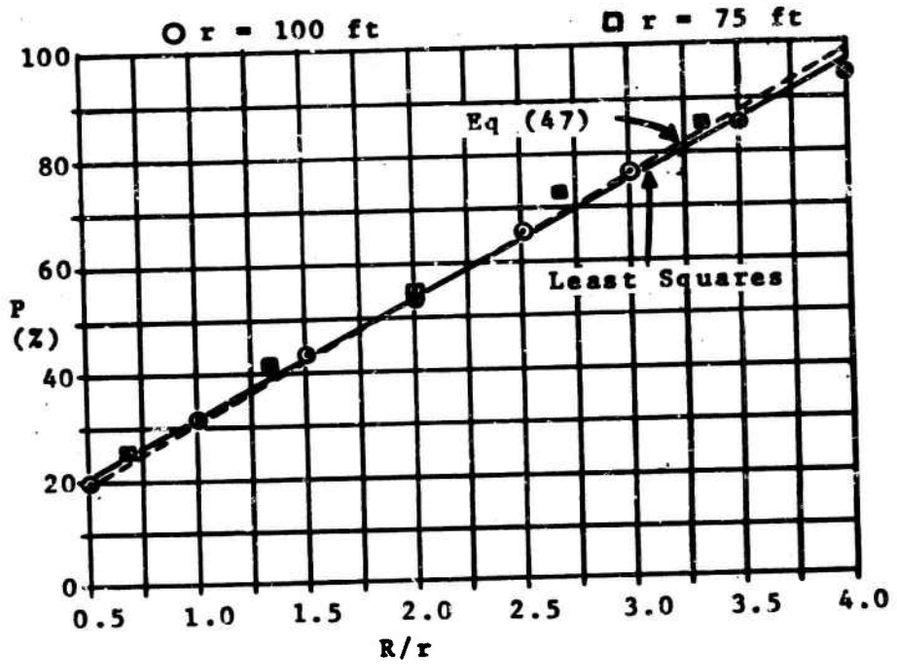

d) P vs R/r at W/V = 0.625

Fig 29 LEAST SQUARES ANALYSIS OF P vs R/r AT VARIOUS W/V (Continued)

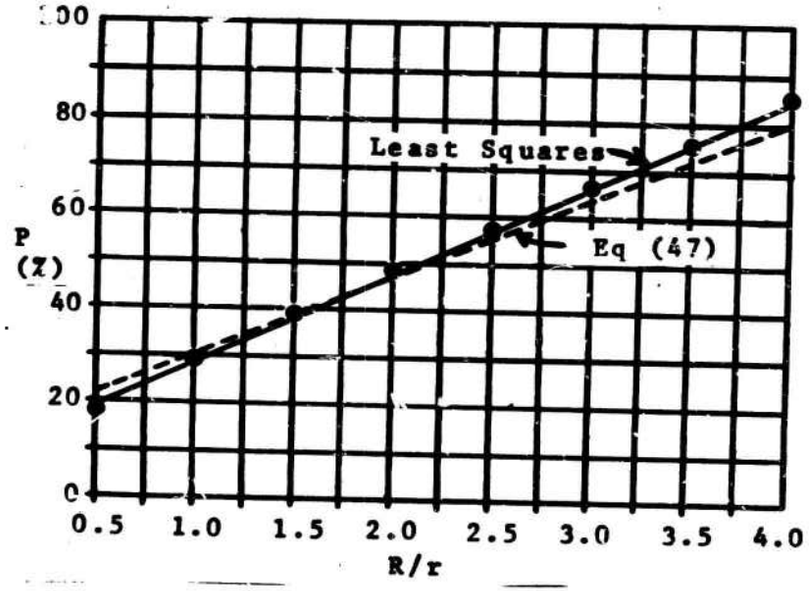

e) P vs R/r at W/V = 0.80

Fig 29 LEAST SQUARES ANALYSIS OF P vs R/r AT VARIOUS W/V (Continued)

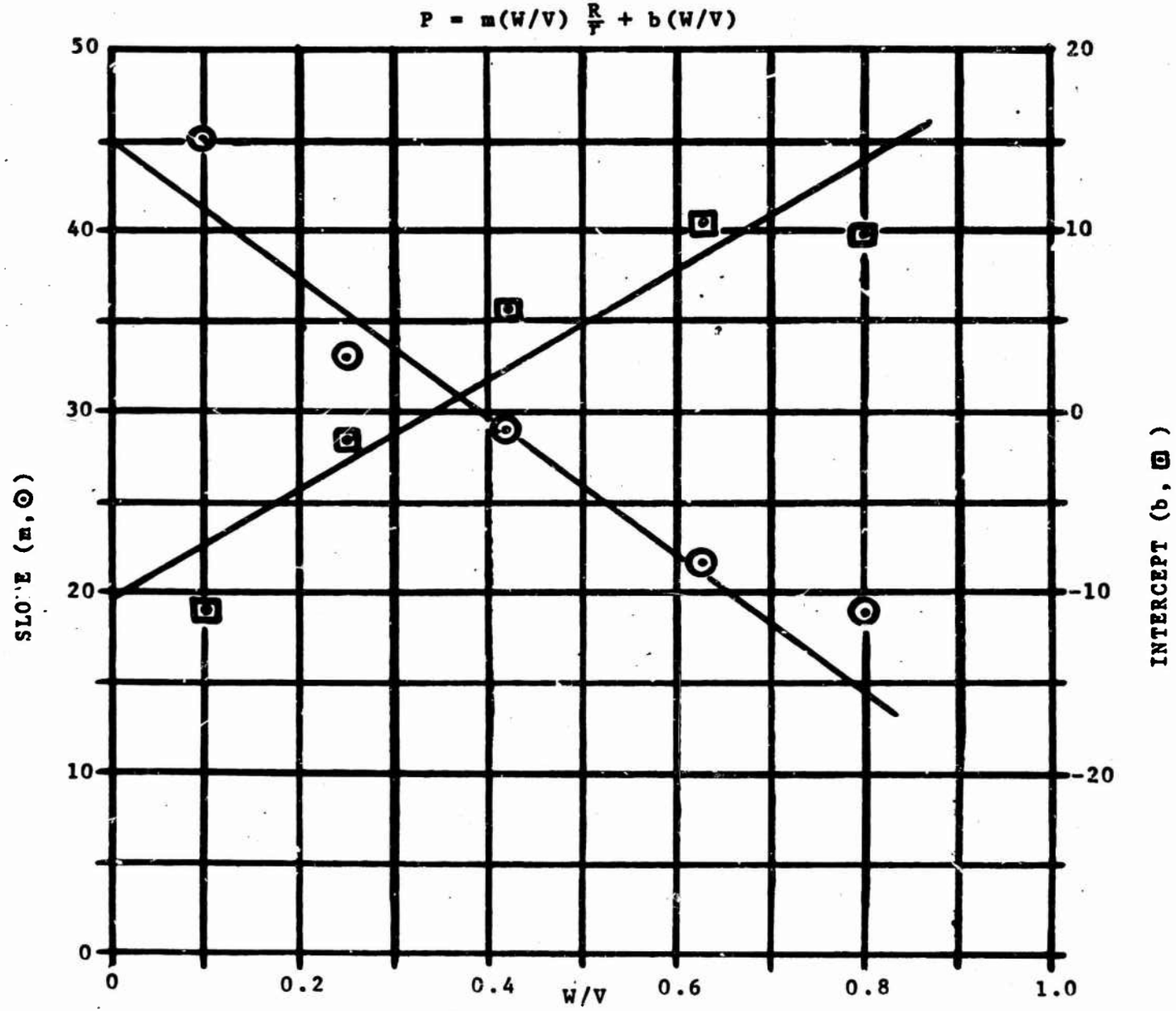

Fig 30 LEAST SQUARES ANALYSIS OF VARIATION OF SLOPE (m) AND INTERCEPT (b) vs W/V FROM RELATION OF P vs R/r

$$R_c/r = \frac{1.70 - 0.84\ W/V}{1.27 - W/V}$$

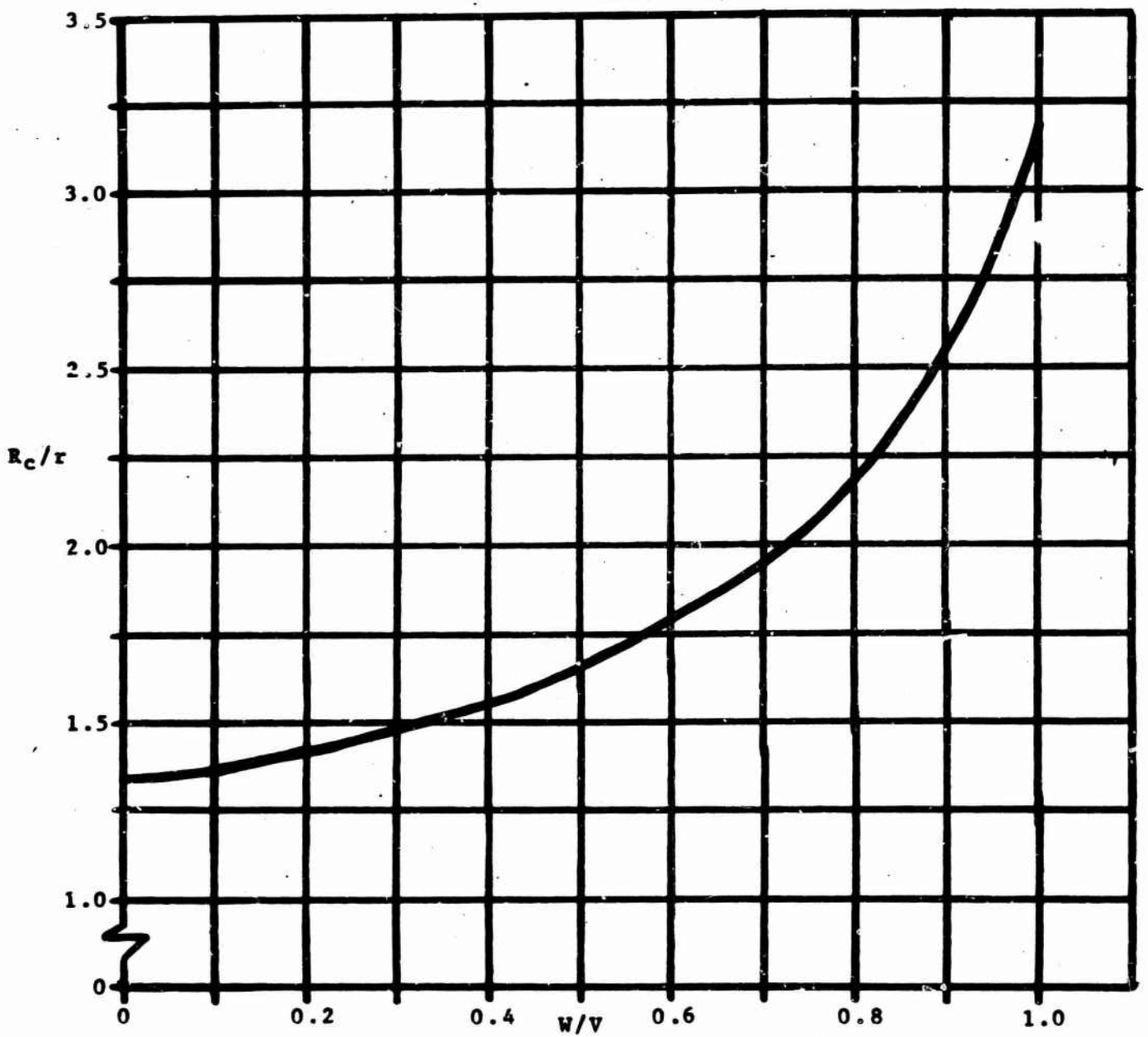

Fig 31 EMPIRICAL RELATION OF R_c/r vs W/V

Unclassified
Security Classification

DOCUMENT CONTROL DATA - R & D

(Security classification of title, body of abstract and indexing annotation must be entered when the overall report is classified)

1. ORIGINATING ACTIVITY *(Corporate author)*
US Army Natick Laboratories
Natick, Mass. 01760

2a. REPORT SECURITY CLASSIFICATION
Unclassified

2b. GROUP

3. REPORT TITLE
Wind Effect on Gliding Parachute Systems with Non-Proportional Automatic Homing Control

4. DESCRIPTIVE NOTES *(Type of report and inclusive dates)*
Research Report

5. AUTHOR(S) *(First name, middle initial, last name)*
Thomas F. Goodrick

6. REPORT DATE	7a. TOTAL NO. OF PAGES	7b. NO. OF REFS
November 1969	55	1

8a. CONTRACT OR GRANT NO.	9a. ORIGINATOR'S REPORT NUMBER(S)
b. PROJECT NO. 1F162203D195	70-28-AD
c.	9b. OTHER REPORT NO(S) *(Any other numbers that may be assigned this report)*
d.	

10. DISTRIBUTION STATEMENT
This document has been approved for public release and sale; its distribution is unlimited.

11. SUPPLEMENTARY NOTES	12. SPONSORING MILITARY ACTIVITY
	US Army Natick Laboratories Natick, Mass. 01760

13. ABSTRACT

Equations are presented and evaluated for estimating the wind effect on the approach path and descending orbit of gliding parachute systems with non-proportional automatic homing control. Exact equations are presented for determining certain characteristic features of the descending orbit. Iteration equations are presented incorporating homing simulation for calculating points at equal time intervals along the ground track. The control response time, effect of deployment position, and impact position probability are discussed. An empirical equation for the radius of the circle of equal probability as a function of turning radius, wind velocity, and system velocity is presented. A parametric analysis of the equations is given for systems with glide ratios from 2.0 to 3.0 and turning radii of 75 ft and 100 ft in winds of from 4 to 32 fps. The analysis shows that accuracy is more dependent on high glide ratio than on turning radius. (U)

DD FORM 1 NOV 68 1473 REPLACES DD FORM 1473, 1 JAN 64, WHICH IS OBSOLETE FOR ARMY USE.

Unclassified
Security Classification

Unclassified
Security Classification

14. KEY WORDS	LINK A		LINK B		LINK C	
	ROLE	WT	ROLE	WT	ROLE	WT
Wind (meteorology)	6					
Gliding	7					
Parachutes	7					
Automatic control	7					
Equations	8,10					
Parameters	8,10					
Impact prediction	4					

Unclassified
Security Classification